Bachelor Thesis

Anomalous warming of sea surface temperature in the Eastern Subtropical North Atlantic
Causes and consequences

Djemila Tassin

Submitted in partial fulfillment of the requirements for the bachelor's degree in marine sciences at the University of Cádiz

Advisers:

Alfredo Izquierdo & Andrés Cianca

Puerto Real, on the 14th September 2018

Acknowledgments

First of all, I would like to thank my tutor and co-tutor, for showing the best support and provide the most accurate guidance and astute advices. Over a hundred emails exchanged, from six different countries, can surely testify of their help and encouragements, but also of the opportunity they gave me to end this life-changing episode with a new adventure, deep into the fields of the Oceanography. Although it is three in the morning and we are still working on it, I have to admit that I received the deepest care from everyone around me during those past 6 months. I would like to express my most profound gratitude to my friends from all over the places and my wonderful roommates, without who this would have, most probably, been a little darker time. To every laugh, tear, beer and help we share with each other's, thank you so much. To my family, who gives me winds to fly towards my dreams and has brought me an unprecedent support during this funny summer, merci. Last but not least, to the person who illuminates my mornings by walking next to me, with her everlasting smile on her pretty face.

Thanks to the staff from every university that I visited, for making my bachelor an unforgettable trip across Europe and more, towards unknown territories, languages and cultures. Thank to Europe and to everyone who works towards a brighter future for our sisters and brothers, and future generations, building a strong community around the values of tolerance, peace and most of all, care for our beloved Oceans.

I would like to thank the Oceanic Platform of the Canary Islands (PLOCAN) and its staff for making freely available the use of this ESTOC data set. I wish to acknowledge use of the Ferret program for analysis and graphics in this paper. Ferret is a product of NOAA's Pacific Marine Environmental Laboratory. (Information is available at http://ferret.pmel.noaa.gov/Ferret/

List of Appendices

Appendix A

Figure 1A. Mean sea surface temperature (ºC) of the Canary Basin for a) SODA reanalysis climatological year and b) DIVA climatology.

Figure 2A. Mean sea surface salinity of the Canary Basin for a) SODA reanalysis climatological year, b) DIVA climatology.

Figure 3A. Mean meridional component of the velocity (m·s-1) over the Canary Basin at 5m for a) SODA reanalysis climatological year and b) DIVA climatology

Figure 4A. Mean zonal component of the velocity (m·s-1) over the Canary Basin at 5m for a) SODA reanalysis climatological year and b) DIVA climatology

Figure 5A. Mean sea surface height (m) of the Canary Basin for a) SODA reanalysis climatological year and b) DIVA climatology

Figure 6A. Wind stress regime for a) winter, b) spring, c) summer, d) autumn. Color key indicates wind stress intensity (N·m2), arrow direction indicates wind stress direction arrow length indicate wind stress magnitude.

Figure 7A. Wind stress (N/m2) field for QuickScat for up left to up right, down left down right = Winter, Spring, Summer, autumn

Appendix B

Figure 1B. ADCP measured directions (v degrees) and intensities (m·s-1) (color key) for a) April and May, b) June, c) July, d) August and e) September.

Figure 2B. SODA climatological directions (degrees) and intensities (m·s-1) (color key) for a) April and May, b) June, c) July, d) August and e) September.

Figure 3B. Mean current direction and intensity for summers (Jun-August) 1997-2017. Data from surface buoy belonging to Puertos del Estado, Gran Canaria coast.

Figure 4B. Mean current direction and intensity for summer 2017 (June-August). Data from surface buoy belonging to Puertos del Estado, Gran Canaria.

Figure 5B. Wind directions and intensities recorded at the ESTOC position (29.2ºN,15.5ºW) from mid-April to late-September. Direction are given in degrees (0º= northerly, 90º= easterly, 180º= southerly,270º= westerly) and intensities in m/s (<0.5 $m \cdot s^{-1}$ - 14 $m \cdot s^{-1}$)

Appendix C

Figures 1C- 12C: SODA climatological SST.

List of acronyms

ESTOC: European Station for Oceanographic Time Series in the Canary Islands
WAC: West African Coast
ADCP: Acoustic Doppler Current Profiler
SODA: Simple Ocean Data Assimilation
CC: Canary Current
AzC: Azores Current
NEC: North Equatorial current
CuC: Canary Upwelling Current
NACW: North Atlantic Central Waters
AAIW: Antarctic Intermediate Waters
NADW: North Atlantic Deep Waters
MW: Mediterranean Waters
DIVA: Data-Interpolating Variational Analysis
GLORYS: Global Ocean Reanalysis

ABSTRACT

The Canary Basin, which encloses the subtropical eastern North Atlantic, is dominated in surface waters by the presence of the Azores Current, the Canary Current and the Canary Upwelling Current. Although extensive work has been done in the area to understand the local dynamics, some oceanographical phenomena remain partially unexplained. Following specific events of unusually high sea surface temperature recorded in the Canary Basin during 2017, the causes of this anomaly have been investigated. Here, the starting point is a long-term mooring, the European Station for Time series in the Ocean Canary Islands (ESTOC) which is found north of the Canary Islands. With moored ADCP, surface current velocities, among others, parameters are measured. In this work, a time series from April to September 2017 is used. The observations are analyzed and compared to a climatology based on the Simple Ocean Data Assimilation (SODA) reanalysis. The principal finding is an anomalous northeastward flow, sustained from late April to late September. This flow was found to be in opposition to the usual southwestward Canary Current dominating the open ocean around the Canary Islands. The temperature recorded also showed anomalous maximum values during early summer. Those two anomalies combined are reported as an explanation for the unprecedent bloom of cyanobacteria *Trichodesmium* spp. Around the Canary Islands during 2017. In future studies, it would be very important to study the long-term recurrence of this king of events, due to the strong ecological and social impact of the anomalies recorded.

Key words: SST anomaly, surface currents, Canary Basin, *Trichodesmium* spp., ADCP, Canary Current

RESUMEN

La Cuenca de Canarias engloba el Atlántico Este Subtropical. La dinámica general superficial se encuentra dominada por la presencia de la corriente de Azores, la corriente de Canarias y la corriente Canaria de Upwelling. A pesar de las extensas investigaciones realizadas en el área, algunos acontecimientos específicos no han sido completamente explicados. Unos eventos de calentamiento extremo de la temperatura del agua medida en la Cuenca de Canarias están siendo investigados. La Estación Europea de Series Temporales Oceánicas de Canarias (ESTOC) proporciona series temporales utilizadas con el objetivo de encontrar las causas del evento de subida de las temperaturas superficiales en 2017 (abril-septiembre). Las medidas tomadas de velocidad y dirección de corriente son comparadas con una climatología oceánica realizada a partir del reanalysis SODA (Simple Ocean Data Assimilation). Los principales resultados son: una anomalía de circulación en las aguas superficiales (20-100 m) sostenida durante el periodo de tiempo estudiado y una anomalía positiva en las temperaturas registradas. Se observó una corriente de dirección noreste, en completa oposición con dirección de corriente dominante mostrada por la climatología (SODA) que se presenta como probable responsable del bloom de *Trichodesmium* spp. acontecido en las Islas Canarias ese mismo año. De cara al futuro, es importante resaltar la necesidad de extensivos estudios para optimizar la comprensión de las causas y frecuencias de estos eventos, ya que presentan un importante impacto social y ecológico en la zona afectada.

Palabras claves: anomalía de SST, corrientes superficiales, Cuenca de Canarias, *Trichodesmium* spp., ADCP, Corriente de Canarias

1. INTRODUCTION

Among the achievements of the international ocean program "Joint Global Ocean Flux Study (JGOFS)" whose goal was "*to determine and understand on a global scale the processes controlling the time-varying fluxes of carbon and associated biogenic elements in the ocean, and to evaluate the related exchanges with the atmosphere, sea floor and continental boundaries*", the creation of the several time-series programs during the eighties and nineties could be emphasized (Karl et al., 2003). Among those are the ALOHA (A Long-term Oligotrophic Habitat Assessment) for the Pacific, the BATS (Bermuda Atlantic Time-series Study) for the western North Atlantic and the ESTOC (European Station for Time series in the Ocean Canary Islands) for the eastern North Atlantic. The permanent collection of data at a constant location, in association with regular cruise campaigns that cover an extended geographic area allows scientists to have a better understanding of the mid and long-term variability of the ocean. A good example is the use of several of those stations for the World Ocean Circulation Experiment (WOCE) (Koltermann et al., 2011).

The present work will focus on data collected at the ESTOC to study a particular event observed during 2017. ESTOC is one of the eight multidisciplinary observational programs started during JGOFS. It is located 100 km north of the Canary Islands and about 300 km off the west African coast (WAC), therefore exhibiting open ocean and oligotrophic gyre characteristics (Neuer et al., 2002). ESTOC has been used since 1994 to study several oceanographic processes in the Canary Basin by means of moorings, XBT deployments and on-board measurements (Cianca, 2003).

1.1 Geographic and oceanographic description

The Canary Islands are found within the Canary Basin (Figure 1), loosely defined as 10ºN-40ºN and east of 35ºW (Stramma, 1984; Mason et al., 2011). Throughout the basin, the Canary Current (hereafter CC) flows southward from Madeira to Cap Verde. It connects the eastward-flowing Azores Current (AzC) (i.e. the northern boundary of the North Atlantic Subtropical Gyre (NASG)), to the westward-flowing North Equatorial Current (NEC, Barton, 2008; Arístegui et al., 2009) (Figure 1). The CC forms therefore the eastern boundary of the anticyclonic NASG. It transports approximately 3 Sv (1 Sv = 10^6 m^3s^{-1}) of North Atlantic Central Waters (NACW) southward (Stramma, 1984; Mason et al., 2011). The CC position over the basin oscillates zonally depending on the season. During winter it is found far offshore, near Madeira, while in summer its position is closer to the African coast (Stramma & Siedler, 1988).

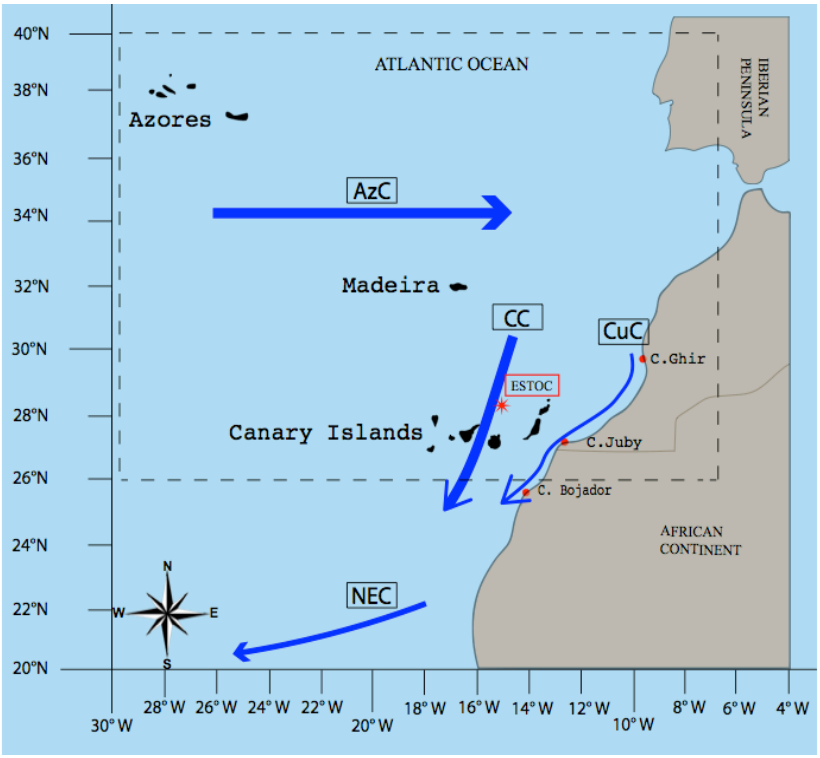

Figure 1. Geographic limits of the Canary Basin. Dotted line indicates the reduced selected area of study. Blue arrows indicate principal currents found in the area. AzC: Azores Current, CC: Canary Current, CuC: Canary Upwelling Current, NEC: North Equatorial Current. Red star indicates the position of the ESTOC station. Red dots over the African continent indicate principal capes relevant for local dynamics.

The northeasterly trade winds dominate across the Canary Basin, blowing alongshore the northwest African coast (hereafter WAC) causing an equatorward surface jet, the Canary Upwelling Current (CuC, Figure 1) (Pelegrí et al., 2005). Trade winds vary seasonally, with maximum intensities during summer (July-August), decreasing in autumn towards winter minimum (Laiz et al., 2012). Ekman transport induced by winds parallel to the coast results in seasonal upwelling of colder NACW from, approximately, 20ºN to 30ºN (Figure 2a) (Van Camp et al., 1991). This appearance of deeper waters in the surface creates a strong temperature gradient off the WAC towards the open ocean. In addition to their seasonal variability, the trade winds also experience inter-annual fluctuations in position and magnitude due to the North Atlantic Oscillation (NAO, Hurrell & Deser, 2010). One way to represent this variability using the NAO index, calculated as the difference in pressure between the Iceland low and the Azores high (Hurrell, 1995). A positive NAO index indicates a stronger meridional mean sea level pressure gradient and an increased zonal atmospheric circulation, resulting in changing patterns of surface air temperature and precipitation over Europe. Positive NAO index also indicates a season of stronger trade

winds, enhanced upwelling and lower sea surface temperature (SST) in the macaronesian Atlantic. On the contrary, negative NAO is related to weaker Azores high, lighter trade winds and warm (positive) SST anomalies (Cropper & Hanna, 2013). The eastern boundary of the NASG is also influenced by upwelling filaments and eddies formation (Johnson & Stevens, 2000).

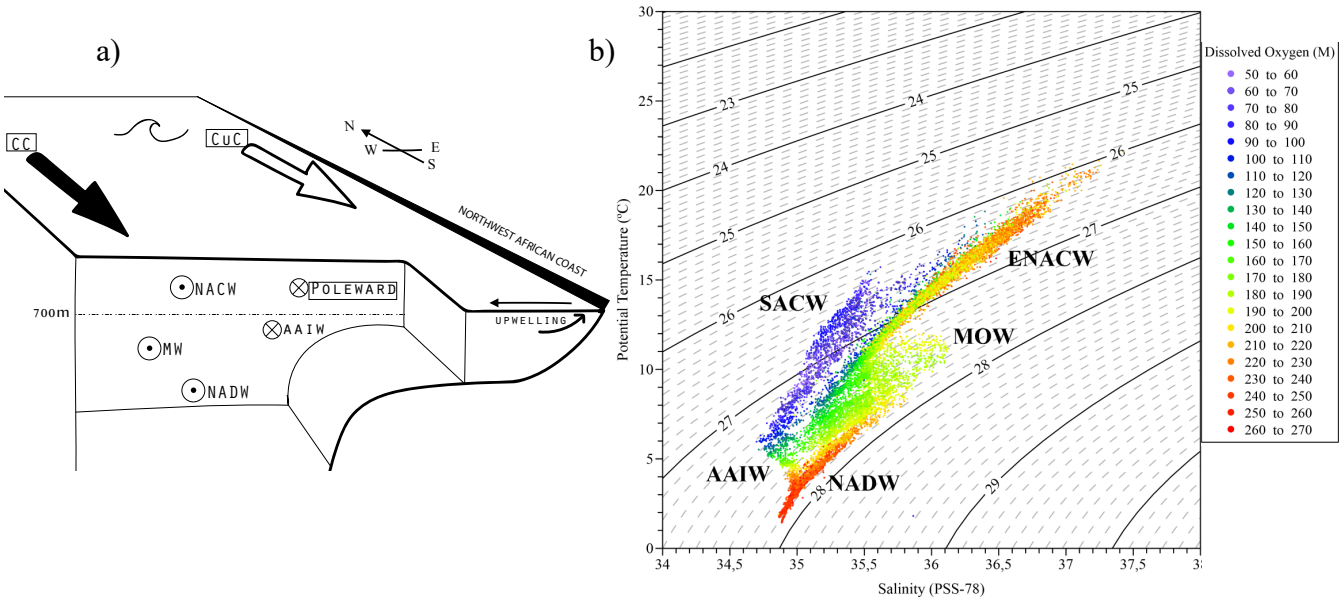

Figure 2. a) Transversal cut of the Canary Basin from surface to bottom at ~26ºN showing local dynamics. Circle with dot stands for southward flow, circle with cross stands for northward flow. b) T-S diagram reflecting water masses present in the Canary Basin (Azevedo et al.,2018) . Color key stands for dissolved Oxygen (M). CC: Canary current; CuC: Canary upwelling current; Poleward: Poleward current centered around 300 m occurring in fall as described by Knoll et al., 2002. Water masses: SACW: South Atlantic Water; ENACW & NACW: (East) North Atlantic Central Water; MOW & MW: Mediterranean (Outflow) Water; NADW: North Atlantic Deep Water; AAIW. Upwelling mechanism of NACW is indicated.

The hydrography of the Canary Basin is characterized by the existing water masses, each one defined by a range of potential temperatures (θ), salinities (S) and dissolved oxygen content (Figure 2b). Surface waters (SF), North Atlantic Central Water (NACW), South Atlantic Central Water (SACW), Antarctic Intermediate Water (AAIW), Mediterranean Water (MW), and North Atlantic Deep Water (NADW) are found (Figure 2a & 2b). The SF occupies the first 150 m where temperature and salinities are principally influenced by wind and solar radiation over a diurnal and seasonal cycle (not shown in figure 2b). NACW is present from the surface down to approximately 700 m (θ,S: 10ºC-18ºC, 35.5-36.5) and is carried by the Canary Current flowing southward (figure 2a) (Hernández-Guerra et al., 2003). SACW θ,S characteristics are 10.5ºC - 35.1. Intermediate waters (700 to 1600 m) are filled by two water masses. On the northern part, MW flows southward from the Gibraltar strait (θ,S: 10ºC, > 35.6). On the southern part, AAIW flows northward, along the African

Coast (θ,S: 7ºC - 8ºC, < 35.4) (Machín et al., 2006). From 1600m to the ocean floor NADW is formed by various types from different origins who share common characteristics (θ,S: 2ºC – 7ºC, ~35.0) (Talley et al., 2011).

1.2 Background and state of the art

Despite a good understanding of the broad dynamics in this area, a more detailed level of knowledge is indispensable to enhance the comprehension of the local dynamics. When studying the Canary Basin, multiple authors found a mean southward flow (~3 Sv) across the Canary Islands [i.e. the Canary Current], but also the existence of a northward flow centered around 300 m during fall between the most oriental islands and the Moroccan coast (Knoll et al., (2002); Machín et al., (2006); Fraile-Nuez et al., (2010); Mason et al., (2011))

Knoll et al. (2002) studied the dynamics of the Lanzarote passage (narrow passage between the islands of Lanzarote and the Moroccan coast) and compared in situ measurements with the fine-resolution CANIGO model of the area (Johnson and Stevens, 2000). They found a mean steady southward flow (few $cm \cdot s^{-1}$) in the surface waters, and the existence of an important reversal to a northward current during fall, occupying the upper 500 m and situated close to the African shelf. Machín et al. (2006) applied an inverse box model to the Canary Basin with data from four hydrographic cruises carried out in the region between Cape Ghir, Madeira Island, and the Canary Islands. They found similar values to Knoll (2002) and Stramma (1984) for the overall transport of the CC (-3.0± 1.0 Sv) and the CuC (-1.0 ± 0.3 Sv). They also found the existence of a northward current in the NACW along the African coast with values of +1.8 ± 0.1 Sv. Fraile-Nuez et al. (2010) studied nine years of mass transport in the Lanzarote passage. What they found was a mean southward transport in the NACW of -0.81± 1.48 Sv, with minimal mass transport in fall, probably due to the flow reversal observed during this season throughout the passage, in agreement with Knoll et al. (2002) and Machín et al. (2006).

Mason et al. (2011) developed a high-resolution climatological numerical study of the Canary Basin using the Regional Oceanic Modeling System (ROMS). Again, the primary solution of the model is a Canary Current transporting around 3 Sv southward. They also exposed a zonal shift of the position of the CC along the year, oscillating from 11º W in winter to 16º W in autumn. Their model also clearly shows the presence of a strong poleward flow centered at a depth of around 300 m along the African Coast.

Regarding winds, Cropper & Hanna (2013) established a trade wind index and used it in correlation with the NAO index to find a statistically significant strength increase of the trade winds over the Macaronesia region (Azores, Madeira, Canary Islands and Cape Verde) from 1973-2013. In addition, they found increasing air temperature across the basin of 0.30–0.38ºC per decade.

Regarding temperatures, Ratsimandresey et al. (2001) described a surface mixed layer for the region reaching more than 22ºC with a maximum depth of 130 m. Likewise, using altimetric (AVRHH) measurements, Vélez-Belchí et al. (2015) investigated the SST trend for the Canary Current Large Marine Ecosystem (40ºN-6ºN, 6ºW-26ºW) from 1982 to 2013. The outcome was a warming trend of mean 0.28ºC decade $^{-1}$ for the region.

1.3 Objectives and hypothesis

Despite the many studies done over the Canary Basin, some features remain partially unexplained. For example, some episodes of anomalously high sea surface temperatures recorded during the past decades around the Canary Islands and most specifically those recorded during spring and summer 2017 (Villagarcia et al., 2018). To deepen in the understanding of those events is the primary objective of this work.

The hypothesis is that an anomalous northward current, as opposed to the usual southward-flowing Canary Current, may be responsible for the unusually high sea surface temperature measured around the Canary Islands.

To answer the hypothesis, the main task of the present work is to analyze the in situ current velocities of the upper thermocline (20-100 m) around the Canary Islands during 2017. The data set used was recorded at the ESTOC time series station (29.17ºN, 15.5ºW) during 2017 (mid-April to September) with an Acoustic Doppler Current Profiler (ADCP).

In order to properly understand the exceptionality of this event observed measurements were compared with climatology created from a 35 year-long reanalysis, the Simple Ocean Data Assimilation (SODA) (Carton et al., 2018).

The methodology and data sets information are explained in sections 2.1-2.2. Validation of the SODA product for the selected domain is provided by comparing it to several other databases in section 2.3. The climatology of the Canary Basin is shown in section 3.1. The complete analysis of the ADCP measurements and its comparison to the climatology is shown at section 3.2, along with a discussion of the results at section 4. Finally, a general review and the conclusion are given in section 5.

2. METHODOLOGY & DATA SETS

The studied area in this paper is the Canary Basin which contains the northern, eastern and southern boundary of the NASG, from 40ºN to 20ºN latitudinally and 6ºW to 30ºW longitudinally (figure 1). For the sake of simplicity, a reduced area of the Canary Basin has been selected (40ºN to 26ºN) which encloses the Azores, Madeira, Salvages and the Canary Islands.

2.1 Programs & methods of analysis

All the data sets were analyzed with Ferret version 6.84. Ferret is an interactive computer visualization and analysis environment designed to meet the needs of oceanographers and meteorologists, distributed and created by the NOAA's Pacific Marine Environmental Laboratory. The Climate Data Operators software (version 1.5.3, Schulzweida (2018), created) was also used for transformation, averaging and other manipulation of the NetCDF files.

For the analysis, the oceanographic convention for directions is used all along the paper (i.e. an easterly current is a water mass flowing towards the east) except for the analysis of wind stress components (Taux, Tauy) were the meteorological convention is used (an easterly wind is a wind blowing from the east). Spectral analyses were computed using Welch's method, applying first a detrend to the entire time-series and using the Hann window for overlapping management. Anomalies were calculated subtracting to each month the long-term mean for the specific month (i.e. mean February was subtracted to every February of the time-series).

2.2 Data sets

In order to establish an oceanic climatology of the Canary Basin, the Simple Ocean Data Assimilation (SODA) reanalysis version 3.3.1 (Carton et al., 2018) was chosen. SODA3 is a university-based ocean-sea ice reanalysis, built around the eddy-permitting Modular Ocean Model v5, ocean component of the Geophysical Fluid Dynamics Laboratory (GFDL) CM2.5 coupled model (Delworth et al., 2012) with technical details as indicated in table 1. Note that SODA does not assimilate velocity information (Carton et al., 2018). Wind stress is calculated from bulk formula Large-Yeager and the forcing fields come from MERRA2 reanalysis (Gelaro et al., 2017). More detailed information about forcing, data assimilation and quality control of the reanalysis can be found online at **http://www.atmos.umd.edu/~ocean/** and also in the related documentation (Carton et al., 2018). For the purpose of the present work, 7 variables were used. Potential temperature (θ, ºC), salinity (unitless, PSS-78), meridional (V, $m \cdot s^{-1}$) and zonal (U, $m \cdot s^{-1}$) components of the

current velocity, sea surface height above geoid (SSH, meters) and finally meridional (Tauy, $N \cdot m^{-2}$) and zonal (Taux, $N \cdot m^{-2}$) wind stress components. The wind stress is the shear stress (i.e. the force) applied by the wind parallel to the surface (water, land) and in the direction of the wind observed at a certain level (10 m above the surface). It is directly calculated from the wind speed. The SODA dataset was obtained from http://apdrc.soest.hawaii.edu/datadoc/soda_3.3.1.php on the 18th June 2018.

SODA has been previously used in multiple other works as for example to study the North Atlantic Oscillation (Groth et al., 2017), to study the tropical instability wave variability in the Atlantic ocean (de Decco et al., 2018), the Pacific Equatorial Undercurrent (Drenkard & Karnauskas, 2014) or to complete long-term moorings measurement around the Madeira islands (Fründt et al., 2013).

In situ data was provided by PLOCAN (The Oceanic Platform of the Canary Islands, http://www.plocan.eu). Data was collected with an Acoustic Doppler Current Profiler (ADCP) NORTEK model Aquadopp 400 kHz at nominal depth of 100 m, moored at the ESTOC (29.19ºN - 15.54ºW), from 14th April 2017 to the 27th September 2017. Measurements were taken every hour (total 3996 time-steps) at 16 depth levels (current profile cell center distance from head (m): 7,12, 17, 22 , 27 ,32 , 37 , 42 , 47 , 52 , 57 , 62 , 67 , 72 , 77 , 82), recording the upper thermocline from nominal depths of 20-100 m, with an accuracy of ±0.5 $cm \cdot s^{-1}$. The upward faced ADCP works by sending a pulse of very high-pitched sound at a constant frequency into the water above it. When the pulse hits a particle, it bounces back to the instrument with a different frequency. The instrument can then measure the difference in frequency between the sent and the received pulse (called the Doppler shift) and use it to calculate the velocity of the water at each desired distance from the ADCP. Final file was provided on a NetCDF format, with the observed velocity speed and direction of current. Vector analysis is delicate; therefore, it has to be decomposed into meridional and zonal components prior to any manipulation.

Components were calculated as follow:

$$U = CSPD \cdot SEN\ (CDIR)$$

$$V = CSPD \cdot COS\ (CDIR)$$

Where U is the zonal component of the velocity (east-west axis, positive flowing towards the east), V is the meridional component of the velocity (north-south axis, positive flowing towards the north), CSPD is the module of the velocity ($m \cdot s^{-1}$) and CDIR is the direction of the velocity vector measured in degrees 0-360º (0º being a current flowing to the north, 180º a current flowing to the south).

Finally, figures 3B and 4B were downloaded from the Spanish Port Authority Portus System, where they provide online information and data obtained from the numerous oceanographic buoys moored along the Spanish coast. The Gran Canaria Buoy was chosen as it is the closest one from the moored ADCP (28.20º N, 15.80º W) (retrieved from http://www.puertos.es/en-us/oceanografia/Pages/portus.aspx on July 20th 2018).

2.3 Validation

To verify de accuracy of SODA3.3.1 for the selected domain, variables used for the climatology were compared with other data sets (table 1).

Table 1: Characteristics of the data sets used to compare the SODA product and validate its accuracy for the selected domain.

	Variables	Resolution and coverage	Assimilated Data	Time range
SODA (Carton et al., 2018)	Temperature, salinity, SSH, Taux, Tauy, U & V	0.5º Global 50 vertical levels	WOD, in situ SST (ICOADS, remotely sensed SST, ARGO profiling floats	1980-2015 Monthly means & 5-day interval average
Diva climatology (Troupin et al., 2010)	Temperature and salinity	0.1º North Atlantic coverage 33 vertical levels	CTD & bottle measurement from WOD05, HydroBase2, ICES, MEDATLAS2, Coriolis & Local Campaigns	Climatological year Monthly means
GLORYS2v4 (Ferry et al., 2012)	U, V & SSH	0.25º Global coverage 75 vertical levels	SST from AVHRR +AMSRE, altimetry from most available satellites, in situ (T, S) from CORIOLIS CORA4.1 data base, CERSAT Sea Ice Concentration	1993-2015 Monthly means
QuikSCAT (Ricciardulli et al., 2011)	Taux, Tauy	0.25º Global coverage	*observed data: microwave scatterometer	1999-2009 monthly means

Temperature and salinity were compared with a high resolution climatology based on the Data-Interpolation Variational Analysis (hereafter DIVA) method, applied to the northeast Atlantic by Troupin et al. (2010). They collected data from several data bases (table 1), eliminated the resulting duplicates and obtained a total of 330,443 profiles which included only CTD and bottle measurements. The result was a high-resolution output grid, with a very good representation of coastal zones and general good agreement with World Ocean Atlas 2005 (Mason et al., 2011). Global mean and climatological monthly values from SODA and DIVA were compared (Figure 1A). They showed general good agreement in their large-scale

magnitudes and ranges, seasonal SST increase, and upwelling mechanism. DIVA showed a higher degree of details (particularly around the islands and the coast), due to its enhanced resolution. The Canary Islands surrounding waters showed similar values, although SODA minima and maxima values were typically 1ºC higher than DIVA. In the SSS field (Figure 2A) SODA showed general good agreement about range and distribution, but DIVA showed more higher resolution features, as fresher water eddy formation around Madeira in March for example.

Meridional and zonal components of the current velocity (V & U) together with the sea surface height (SSH) were compared with the Global Ocean Reanalysis 2v4 (Ferry et al., 2012) (hereafter GLORYS), provided by the Copernicus Marine Environment Monitoring Service (table 1). Average values for surface meridional and zonal velocities show overall good agreement (Figures 3A & 4A respectively). Features like the Azores Current and the WAC upwelling showed very similar patterns. However, some discrepancies exist when comparing both reanalyses at one precise location, with SODA showing more inter-annual variabilities than GLORYS. Both reanalyses also agreed quite well over distribution and values of sea surface height. (Figure 5A).

Finally, the meridional and zonal components of the ocean surface wind stress (Taux, Tauy) were compared with data from QuikSCAT satellite (table 1) (Ricciardulli et al., 2011) available online at www.remss.com/missions/qscat, (accessed 18th June 2018).

SODA and QuickScat agree quite well over the directions and intensities of the wind stress vector for seasonal variations (Figures 6A & 7A respectivelly). SODA shows however a smaller range of intensities because it doesn't model the local effects of islands and coastal morphologies over wind speed while QuickScat captures the influenced of coastal areas over wind speeds.

3. RESULTS

3.1 SODA Climatology

The mean state, the seasonal variability and the long-term variability of the above-mentioned variables are described hereafter.

Sea surface temperature (SST), sea surface salinity (SSS), sea surface height (SSH), currents and wind stress show a common spatial pattern reflecting the anticyclonic shape of the NASG (see Figures 1A, 2A, 3A, 4A, 5A). SST, SSS and SSH increase from NE to SW over most of the domain, with isolines turning parallel to the coast when reaching western Africa. Prevailing trade winds blow from the N-NE, parallel to the Iberian and African coasts. The surface current field is dominated by the westward Azores current in the north of the domain and the equatorward Canary Current off the African coast. The upwelling effect along the WAC is seen in every variable studied. SST, SSS and SSH show an important decrease over the transition zone from open ocean to coastal waters, with the Canary Islands located in an area with strong gradients. Additionally, current velocities and wind stress show strong alongshore intensification of flow (both along the WAC and the Iberian Peninsula), with the southward wind stress resulting in southward current jet and eastward Ekman transport (upwelling effect).

SST, SSS and SSH present a similar annual cycle principally influenced by the solar radiation (Figure 3a, 3b, 3c). Minimum values appear in spring, when the surface waters radiate more energy than they receive, resulting in colder waters (15 ºC - 21 ºC), low salinities (35.9 - 37.0) and low sea surface height (-0.36 m to -0.22 m) due to thermal contraction of the water. Autumn shows maximum SST (21ºC to 25.5ºC), SSS (36.2-37.1) and SSH (-0.028 m to -0.1 m). Wind stress also shows an annual cycle, with stronger northerlies trade winds during summer (Figure 3d, wind stress maximum in July, around 0.07 $N \cdot m^{-2}$), especially south of 36ºN and along the WAC, and weaker northeasterly during winter (wind stress minimum in November, around 0.02 $N \cdot m^{-2}$). The Azores current (seen in Figure 3e by a positive (eastward) zonal jet centered at 34ºN) is stronger in winter (0.08 $m \cdot s^{-1}$) and weaker during summer (0.01 $m \cdot s^{-1}$). The CC (Figure 4f), to a large extent fed by the AzC, by mass conservation reasons presents its minimum velocities at the same time (summer, 0.02 $m \cdot s^{-1}$ southward) and maximums during spring (0.016 $m \cdot s^{-1}$ southward). Summer corresponds to slower AzC and CC but in contrast to strong trade winds south of 32º and along the WAC causing maximum upwelling (westward (negative) zonal flow, 0.07 $m \cdot s^{-1}$).

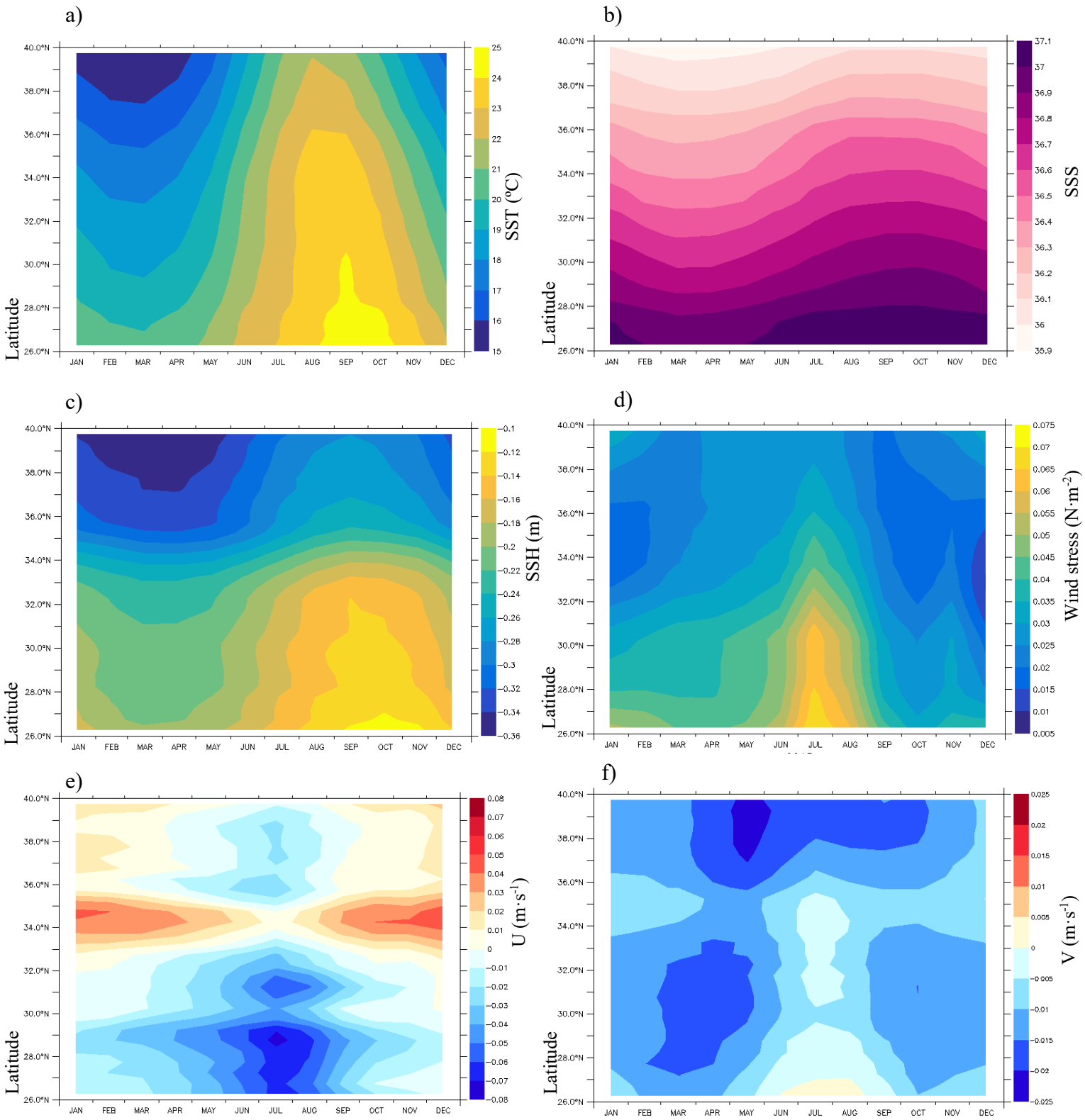

Figure 3. SODA climatology for a) SST (ºC), b) SSH, c) SSH (m), d) wind stress ($N \cdot m^{-2}$), e) U (zonal component of the velocity, $m \cdot s^{-1}$), f) V (meridional component of the velocity, $m \cdot s^{-1}$).

The long-term variability based on summer months (May to September) of U and V at the ESTOC coordinates shows interesting results (Figure 4). The zonal component of the velocity is mostly positive (eastward, 0 - 0.05 $m \cdot s^{-1}$) for the entire time series with some intense positive pulses (around 0.2 $m \cdot s^{-1}$) as for example summer 1990, 1997 and 2003. Vertically, there is homogeneity of the water column except for upper most layers (0-15 m) which show principally negative (westward) values over the entire period. Meridional component of the velocity (Figure 4) is mostly negative (0 - 0.4 $m \cdot s^{-1}$) but shows positive (northward) pulses from 1985 to 2005, especially during summer 1994. Vertically, values are mostly homogenous. Spectral analysis revealed significant peaks at 25.9 and 4.5 months for zonal velocities and 17. 9 and 4.5 months for meridional velocities.

To further understand the relationship between both surface currents and temperature anomalies, correlation coefficients (r) were calculated for long-term anomalies at the ESTOC corresponding location (table 2).

Table 2: Correlation coefficient (r) for temperature anomalies versus other variables

	TAUX anomalies	TAUY anomalies	U anomalies	V anomalies
Temperature anomalies	0.2569	0.2530	0.3686	0.1188

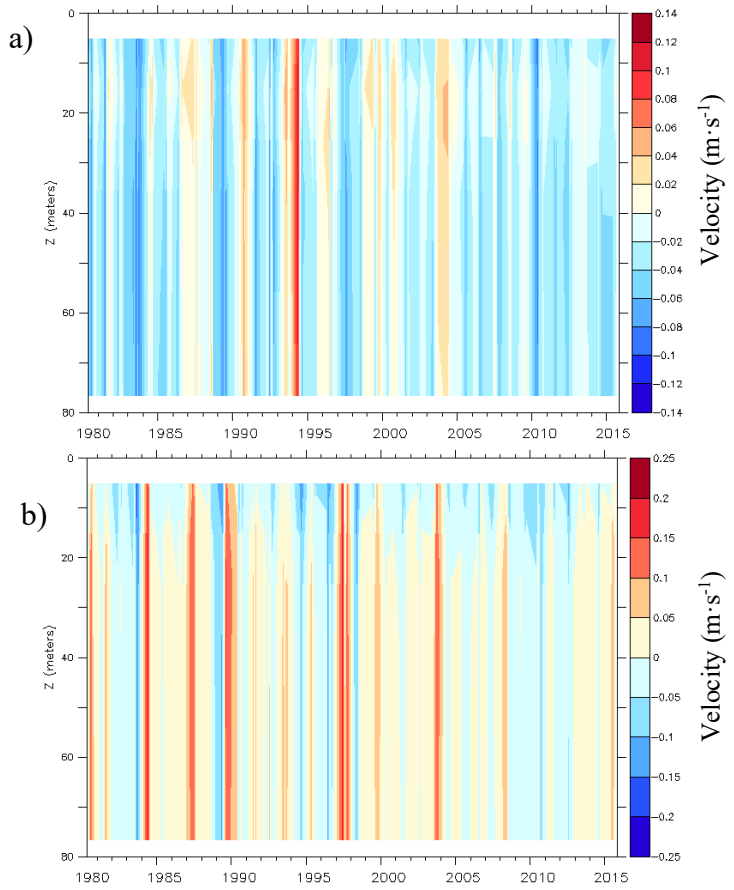

Figure 4. a) SODA meridional component of the velocity ($m \cdot s^{-1}$). Red (blue) indicates northward (southward) velocities, b) SODA zonal component of the velocity ($m \cdot s^{-1}$), Red (blue) indicates eastward (westward) velocities. Only summer months (May-Sep) from 1980 to 2015.

3.2 ADCP vs SODA

Hovmoller diagrams show evolution in time and depth of velocities measured by ADCP versus velocities modeled by the SODA climatology (Figures 5a ADCP, 5b SODA).

ESTOC ADCP measurements show that the zonal component of velocity (Figure 5a) was positive (flowing eastward) over most of the time range, except for 3 negative peaks during April, mid-May and a longer peak late-July, where flow reverse westward. Mean daily maximum intensities were measured late June centered at 40 m (0.2 $m \cdot s^{-1}$). The water column behaved homogenously except for the upper layer (20-30 m) which exhibits a different pattern, more often maintaining positive values but experiencing the July negative peak earlier in time.

The climatological zonal component of current velocity, according to SODA (Figure 5b), shows a quite different pattern, where a subsurface layer (0-20 m) always has negative values (westward flow). Deeper layers exhibit instead negative values from April to June and slightly positive values (eastward, 0.01 $m \cdot s^{-1}$) for July, August and September. When comparing ADCP to SODA, they both agree about the heterogeneity between the upper layers and the deeper ones.

ADCP measured meridional velocity (Figure 5a') shows drastic inversion from fast negative (southward) to fast positive (northward) values in April, then mostly negative values for May, June and July and essentially positive values for August and September. Like for the zonal component, the meridional velocity shows a different pattern over the upper layer (20-30 m) with primarily positive values over the entire time range.

SODA climatological meridional velocity (Figure 5b') displays continuously negative values (southward). However, there is a near-surface core (10m-30 m) with slower than surrounding velocities from May to September, with three very small patches of positive velocities. When comparing ADCP 2017 data versus SODA climatology, it can be seen that meridional velocities are overall similar for May, June and July although ADCP measurements oscillate a few times towards positive values, which is not the case in SODA. Strongest disagreements appear for: April, with a measured very positive peak (northward); August and September with a totally opposed direction of flow (northward for ADCP, southward for SODA). The range of ADCP measured velocities are consistent with the ranges shown by the SODA reanalysis long-time series (Figure 4).

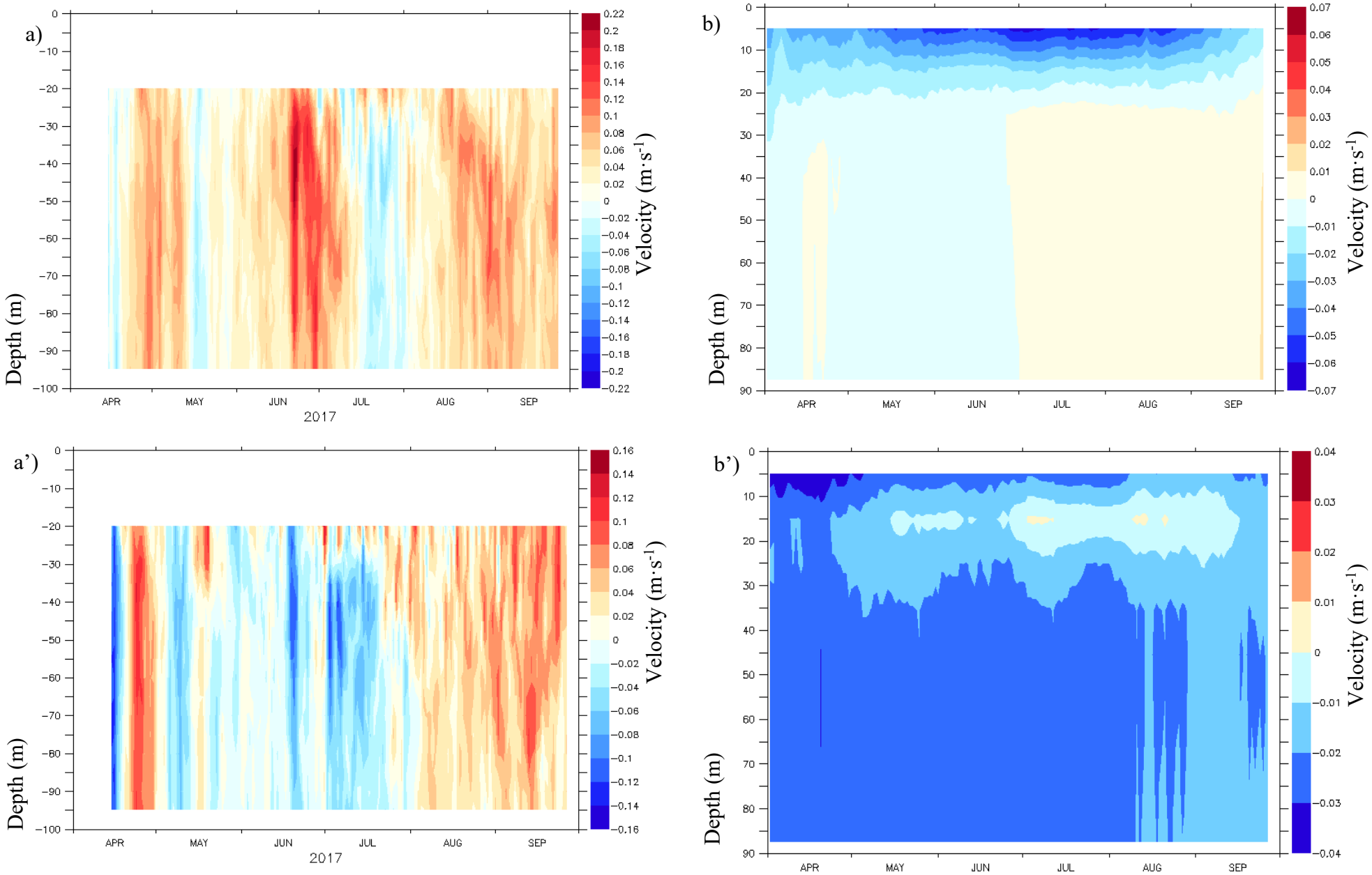

Figure 5. Top: Zonal component of the velocity ($m \cdot s^{-1}$), evolution in time and depth at 29.2º N, 15.5º W, from a) ADCP measurements, b) SODA climatology. Bottom: Meridional component of the velocity ($m \cdot s^{-1}$), evolution in time and depth at 29.2º N, 15.5º W from a') ADCP measurements, b') SODA climatology

Globally, the ADCP recorded several anomalous behaviors for both components of the surface velocity. The meridional component showed inverted directions during late April, August and September, while the zonal component showed inverted directions from mid-April to mid-May and then late-May to mid-July. Both components showed sustained positive velocities (eastward and northward) across the upper layers registered (20-30 m)

A more intuitive way to see the extension of the anomalous event is to represent the resulting current direction and its intensities (Figure 6a). Most of the time (70% of days), daily mean current was measured flowing NNE to SSE (mean 68.5º). Current was also measured flowing southwestward and northwestward, but only a small portion of days. Maximum frequencies were recorded flowing northeastward. Mean daily speed of current measured was 0.074m·s^{-1}.

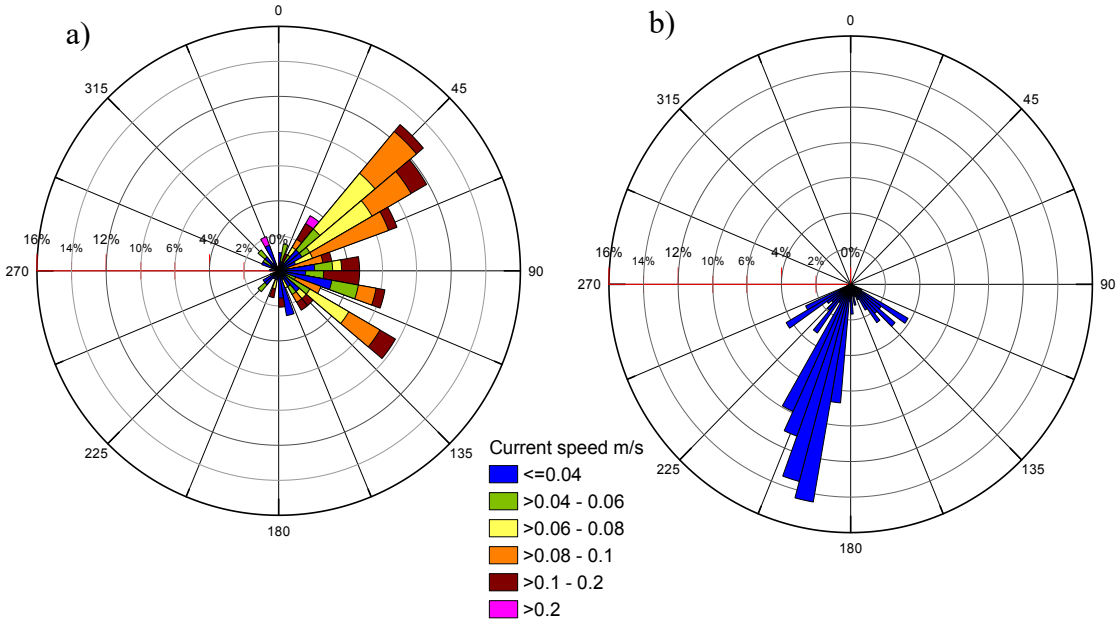

Figure 6: Current directions and velocities (color). Frequencies in % of total days for a) ADCP measurements and b) SODA climatological year. Depth averaged (20 to 100 m). Direction are given in degrees (0º= northward, 90º=eastward, 180º=southward, 270º=westward) and intensities in m·s^{-1} (<0.04 m·s^{-1} to >0.2 m·s^{-1}).

In opposition to the ADCP measured directions, SODA (Figure 6b) climatological year is completely dominated by the SW direction. Comparing ADCP measurements to SODA month-to-month (Figures 2A & 2B) clearly shows that 2017 experienced an anomalous direction of the surface current. July shows the smallest discrepancies between ADCP and SODA. The other months show a very different pattern between ADCP (pointing mostly NE) and SODA (pointing mostly SSW) with April, August and September showing the greatest disparities.

Long-term summer measurements (June-August 1997-2017) from a surface buoy near Gran Canaria (technical details in section 2.3) (Figure 3B) indicate that over the past 20 summers, current flew more often southwestward but also reversed northeastward. However, the buoy may be subject to local dynamics created by the islands influence, which could induce a natural variability somehow different from the ESTOC dynamic. Nevertheless, for 2017 (Figure 4B), the surface buoy record agrees quite well with the ADCP record. Half of the time, current was measured pointing between N and SE and maximum frequencies were measured NNE.

To summarize, the ADCP measurements at the ESTOC location from April to September 2017 are found to exhibit an anomalous pattern of reversed direction of current velocity when they are compared to the established climatology (SODA). Moreover, the anomalous pattern agrees with the one recorded during 2017 at a surface buoy near Gran Canaria.

The temperature recorded with the ADCP (at nominal depth 105 m) also showed records which are above the seasonal temperatures showed by the SODA climatology (Figure 7). Measured temperatures show oscillating values from mid-April to June (18.47ºC±0.19ºC), which agree with the tendency showed by the SODA climatology. However, early-July temperatures increased to reach maximum values (daily mean: 18.88ºC) while SODA shows in contrast minimum annual values (18.1ºC). Even more, ADCP measurements were above the SODA long-term variability (mean + one standard deviation). After the July peak, temperatures rapidly decreased to match the climatological tendencies again.

Winds were also recorded at the ESTOC during the time interval of the moored ADCP. Measurements indicate predominant northeasterly (trade winds) during the entire period of time (Figure 5B), blowing from 0 to 12 $m \cdot s^{-1}$.

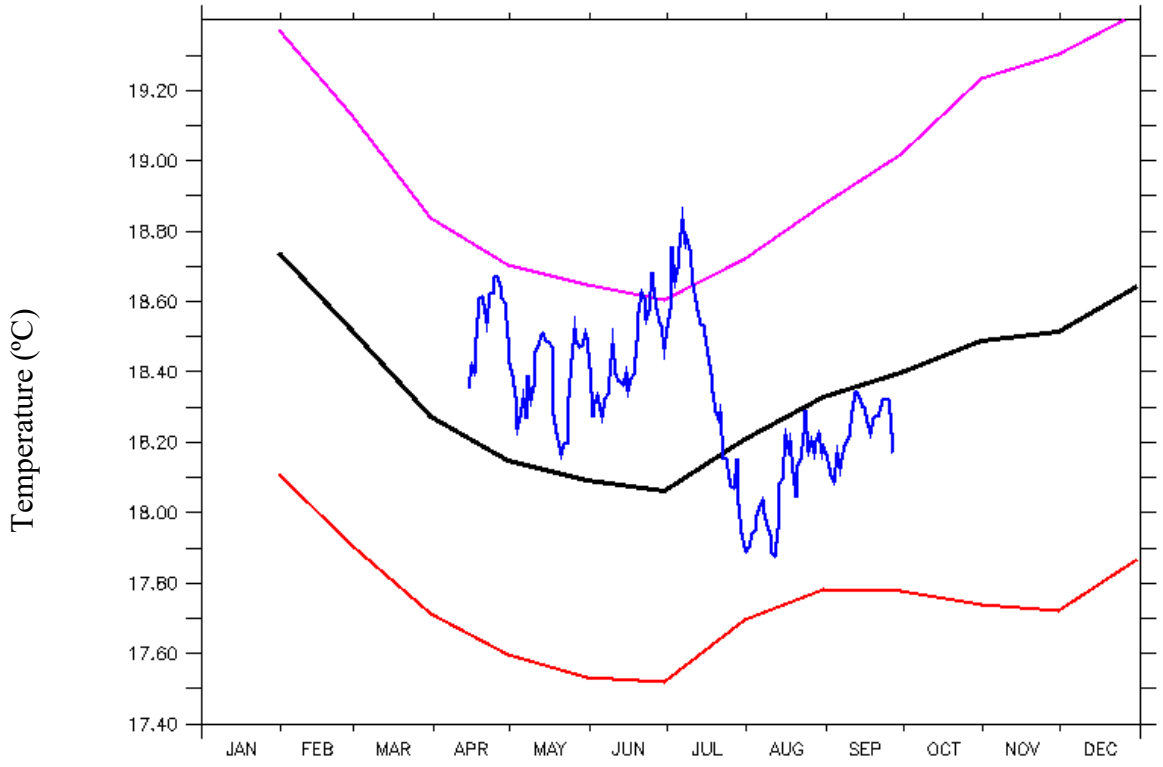

Figure 7: Water temperature (ºC) at 100 m depth. Blue curve: temperature measured with ADCP, black curve: SODA climatological temperature, red curve: SODA - 1standard deviation, pink curve: SODA + 1 standard deviation. Maximum blue peak during July shows the anomaly event, where measured temperatures were above SODA variability.

4. 1 Discussion

The initial hypothesis was that an anomalous northward current, as opposed to the usual southward-flowing CC, was responsible for the surface warming in the Canary basin in spring and summer 2017. After extensively comparing in situ measurements with the SODA reanalysis climatology, it was shown that 2017 experienced indeed, currents quite different from the "mean state". The results of the ADCP measurements revealed a period of currents flowing predominantly to the NE, especially during April, August and September, while the SODA climatology showed south and southwestward current as the "mean state" for the period of time (April-September) and location compared (ESTOC).

Based on the climatology provided in section 3.1, warming of surface waters occurs gradually from southwest to northeast during summer months over the basin due to radiation annual cycle. Hence, if surface waters are transported northeastward they will cause an advective additional warming around the Canary Islands, whose eastern edge is normally under the influence of upwelled colder waters from the African coast. This could have some important effect over the fauna and flora of the area, due to the increase in surface waters temperature.

The temperature measured shows indeed a peak of anomalously high temperature (> 18.6ºC) maintained from late-June to early-July. Simultaneously, the Canary Islands experienced during summer 2017, a strong bloom of *Trichodesmium* spp., a colonial cyanobacterium which present optimal development at temperatures between 24ºC and 30ºC (Breitbarth et al., 2007), naturally selected when strongly stratified waters and high iron input (Tyrrell et al., 2003) and most abundant around equatorial latitudes (Fernández et al., 2010). Arístegui and others published a report about the presence and development of *Trichodesmium* spp. around the Canary Islands during summer 2017 (Arístegui et al., 2017). They analyzed SST from the surface buoy of Gran Canaria and Tenerife and found that June experienced 23.3ºC, which is enough for the cyanobacteria to develop and warmer than the climatic mean of XXXX, and that May and July 2017 had had maximum SST compared to any May or July since 1997. Combined to weak trade winds that enhance stratification and frequent input of Saharian dust (with high content of iron and phosphates), those 3 parameters produce very good conditions for *Trichodesmium* spp. filaments to grow and persist, as it already happened with similar conditions in 2004 (Ramos et al., 2005). The observations revealed by the surface buoy in Gran Canaria

allows us to ensure the similarity of conditions happening simultaneously at the ESTOC and around the Canary Islands.

With all the above in mind, it can realistically be inferred that the anomalous northeastward current detected by the ADCP may have help to maintain the water temperature above what is necessary for the cyanobacteria bloom to persist. Moreover, SODA reanalysis showed weak but positive coefficient of correlation between zonal component of current anomalies and temperature anomalies (r=0.37). However, it is delicate to ensure the relationship between northeastward current and anomalously high temperatures due to the influence of many other factors involved in regulating the water temperature (e.g. wind stress). It is also important to keep in mind that the comparison is done with SODA reanalysis which is, nevertheless, only a model of the reality and by this, it may reproduce erroneously some features, most probably due to its restricted spatial resolution. Notwithstanding, some authors are alerting about the occurrence of a "tropicalization" of the Canary Islands oceanic climate, in particular due to the increase in tropical species found in coastal waters (Brito et al., 2005). Environmental changes, as water temperature warming causing northward displacement of subtropical species (Philippart et al., 2011) combined with adequate wind and Saharian dust conditions could explain why the Canary Islands suffered blooms of *Trichodesmium* spp. in 2004, 2011 and 2017. Furthermore, the sustained northeastward transport of surface waters may have favor *Trichodesmium* spp., which are found in considerable concentrations west and southwest of the islands (McCarthy & Carpenter, 1979; Tyrrell et al., 2003; Mompeán et al., 2013) to bloom by displacing them towards an optimal environment.

Another important feature of the results of the mooring measurements is the complete absence of "usual" southwestward flow during August and September 2017. The first reason one could think to explain this "reversed flow" would be due to the influence of the wind stress, which forces the current under it, but surprisingly the wind pattern observed at the ESTOC location was consistent with the regular trade winds direction (northeasterly). When analyzing the long-term summers (May to September) from SODA reanalysis (see section "climatology"), it is evident that this type of "reversed" flow has happened before. SODA reanalysis not only revealed complex variation/fluctuation of currents directions and intensities within the selected

domain (surface versus depth, costal versus open ocean, the upwelling influence …) but also all along the 35 years of the model, which could, together, explain some of the discrepancies/variability observed during 2017. Although the simple spectral analysis did not reveal any multi-year periodic cycle, it would then be interesting, but out of context for this research, to study more intensely the existence of a periodicity of this kind of events. For example, during the analysis of SST on the southeastern north Atlantic, Borges et al. (2004) found a 4-years period increase of maximum SST and decrease of minimum SST two years later, but only regarding areas belonging to the coastal transition zone of the eastern boundary current of the NASG, principally northeast of Lanzarote and south of the Canary Islands. Lastly, it would also be interesting to study the SSH variation over the entire selected domain for the duration of the anomalous current flow to determine the spatial extent of the event.

5.1 CONCLUSION

1. A particular event of high SST in the Canary Islands during 2017 motivated the analysis of in situ current velocities, with the hypothesis of an anomalous circulation event responsible for the SST increase. The analysis revealed a sustained north-eastward flow which is in opposition to the usual southwestward flow found in the area. The finding supports the initial hypothesis, with the difference of a northeastward instead of a northward flow. The correlation between the anomalous circulation and water temperatures increment was discussed and proposed as an explanation for the blooms of cyanobacteria *Trichodesmium* spp. around the Canary Islands during summer 2017. Here, the transport northeastward of warm southern waters was exposed as a possible factor causing higher-than-usual water temperatures which better the conditions for the cyanobacteria to bloom. Furthermore, the possible displacements of *Trichodesmium* spp. northeastward by the surface current shift may have carried them to an area of improved blooming conditions.

2. Secondly, the wind stress was investigated as a possible cause for the reversed current direction but no anomaly within the wind direction was detected.

3. Finally, the question of periodicity of this kind of events was posed but left unanswered, leaving an open door for further investigation into the subject.

Reference

Arístegui, J., Barton, E. D., Álvarez-Salgado, X. A., Santos, A. M. P., Figueiras, F. G., Kifani, S., Hernández-León, S., Mason, E., Machú, E., & Demarcq, H. (2009). Sub-regional ecosystem variability in the Canary Current upwelling. *Progress in Oceanography*, *83*(1–4), 33–48. https://doi.org/10.1016/j.pocean.2009.07.031

Arístegui, J., González-Ramos, A. J., & Benavides, M. (2017). *Informe sobre la presencia de Trichodesmium spp. en aguas de Canarias, en el verano de 2017.* las palmas de Gran canaria. https://doi.org/10.1787/9789264097780-3-es

Barton, E. D. (2008). Canary and Portugal Currents. *Encyclopedia of Ocean Sciences: Second Edition*, 467–476. https://doi.org/10.1016/B978-012374473-9.00360-X

Borges, R., Hernández-Guerra, A., & Nykjaer, L. (2004). Analysis of sea surface temperature time series of the south-eastern North Atlantic. *International Journal of Remote Sensing*, *25*(5), 869–891. https://doi.org/10.1080/0143116031000082442

Breitbarth, E., Oschlies, A., & LaRoche, J. (2007). Physiological constraints on the global distribution of *Trichodesmium* - Effect of temperature on diazotrophy. *Biogeosciences*, *4*(1), 53–61. https://doi.org/10.5194/bg-4-53-2007

Brito, A., Falcón, J. M., & Herrera, R. (2005). Sobre la tropicalización reciente de la ictiofauna litoral de las islas Canarias y su relación con cambios ambientales y actividades antrópicas. *Vieraea*, *33*, 515–526.

Carton, J. A., Chepurin, G. A., & Chen, L. (2018). SODA3: A New Ocean Climate Reanalysis. *Journal of Climate*, *31*(17), 6967–6983. https://doi.org/10.1175/JCLI-D-18-0149.1

Cianca, A. (2003). Agua central noratlántica. Modos y variabilidad en el atlántico centro oriental (ESTOC). PhD dissertation. University of Las Palmas de Gran Canaria, Las Palmas, Spain.

Cropper, T. E., & Hanna, E. (2013). An analysis of the climate of Macaronesia, 1865-2012. *International Journal of Climatology*, *34*(3), 604–622. https://doi.org/10.1002/joc.3710

de Decco, H. T., Torres Junior, A. R., Pezzi, L. P., & Landau, L. (2018). Revisiting tropical instability wave variability in the Atlantic ocean using SODA reanalysis. *Ocean Dynamics*, *68*(3), 327–345. https://doi.org/10.1007/s10236-017-1128-2

Delworth, T. L., Rosati, A., Anderson, W., Adcroft, A. J., Balaji, V., Benson, R., Dixon, K., Griffies, S. M., Lee, H. C., Pacanowski, R. C., Vecchi, G. A., Wittenberg, A. T., Zeng, F.,

& Zhang, R. (2012). Simulated climate and climate change in the GFDL CM2.5 high-resolution coupled climate model. *Journal of Climate*, *25*(8), 2755–2781. https://doi.org/10.1175/JCLI-D-11-00316.1

Drenkard, E. J., & Karnauskas, K. B. (2014). Strengthening of the pacific equatorial undercurrent in the SODA reanalysis: Mechanisms, ocean dynamics, and implications. *Journal of Climate*, *27*(6), 2405–2416. https://doi.org/10.1175/JCLI-D-13-00359.1

Fernández, A., Mouriño-Carballido, B., Bode, A., Varela, M., & Marañón, E. (2010). Latitudinal distribution of *Trichodesmium* spp. and N2fixation in the Atlantic Ocean. *Biogeosciences*, *7*(10), 3167–3176. https://doi.org/10.5194/bg-7-3167-2010

Ferry, N., Parent, L., Garric, G., Bricaud, C., Testut, C.-E., Le Galloudec, O., Lellouche, J.-M., Drevillon, M., Greiner, E., Barnier, B., Molines, J.-M., Jourdain, N. C., Guinehut, S., Cabanes, C., & Zawadzki, L. (2012). GLORYS2V1 global ocean reanalysis of the altimetric era (1992-2009) at meso scale. *Mercator Quarterly Newsletter*, *44*, 29–39.

Fraile-Nuez, E., MacHín, F., Vélez-Belchí, P., López-Laatzen, F., Borges, R., Benítez-Barrios, V., & Hernández-Guerra, A. (2010). Nine years of mass transport data in the eastern boundary of the North Atlantic Subtropical Gyre. *Journal of Geophysical Research: Oceans*, *115*(9). https://doi.org/10.1029/2010JC006161

Fründt, B., Müller, T. J., Schulz-Bull, D. E., & Waniek, J. J. (2013). Long-term changes in the thermocline of the subtropical Northeast Atlantic (33°N, 22°W). *Progress in Oceanography*, *116*, 246–260. https://doi.org/10.1016/j.pocean.2013.07.004

Gelaro, R., McCarty, W., Suárez, M. J., Todling, R., Molod, A., Takacs, L., Randles, C. A., Darmenov, A., Bosilovich, M. G., Reichle, R., Wargan, K., Coy, L., Cullather, R., Draper, C., Akella, S., Buchard, V., Conaty, A., da Silva, A. M., Gu, W., Kim, G. K., Koster, R., Lucchesi, R., Merkova, D., Nielsen, J. E., Partyka, G., Pawson, S., Putman, W., Rienecker, M., Schubert, S. D., Sienkiewicz, M., & Zhao, B. (2017). The modern-era retrospective analysis for research and applications, version 2 (MERRA-2). *Journal of Climate*, *30*(14), 5419–5454. https://doi.org/10.1175/JCLI-D-16-0758.1

Groth, A., Feliks, Y., Kondrashov, D., & Ghil, M. (2017). Interannual variability in the North Atlantic Ocean's temperature field and its association with the wind stress forcing. *Journal of Climate*, *30*(7), 2655–2678. https://doi.org/10.1175/JCLI-D-16-0370.1

Hernández-Guerra, A., Fraile-Nuez, E., Borges, R., López-Laatzen, F., Vélez-Belchí, P., Parrilla,

G., & Müller, T. J. (2003). Transport variability in the Lanzarote passage (eastern boundary current of the North Atlantic subtropical Gyre). *Deep-Sea Research Part I: Oceanographic Research Papers*, *50*(2), 189–200. https://doi.org/10.1016/S0967-0637(02)00163-2

Hurrell, J. W. (1995). Decadal trends in the North Atlantic oscillation: Regional temperatures and precipitation. *Science*, *269*(5224), 676–679. https://doi.org/10.1126/science.269.5224.676

Hurrell, J. W., & Deser, C. (2010). North Atlantic climate variability: The role of the North Atlantic Oscillation. *Journal of Marine Systems*, *79*(3–4), 231–244. https://doi.org/10.1016/j.jmarsys.2009.11.002

Johnson, J., & Stevens, I. (2000). A fine resolution model of the eastern North Atlantic between the Azores, the Canary Islands and the Gibraltar Strait. *Deep-Sea Research Part I: Oceanographic Research Papers*, *47*(5), 875–899. https://doi.org/10.1016/S0967-0637(99)00073-4

Karl, D. M., Bates, N. R., Emerson, S., Harrison, P. J., Jeandel, C., Llinâs, O., Liu, K.-K., Marty, J.-C., Michaels, A. F., Miquel, J. C., Neuer, S., Nojiri, Y., & Wong, C. S. (2003). Temporal Studies of Biogeochemical Processes Determined from Ocean Time-Series Observations During the JGOFS Era. *Ocean Biogeochemistry*, 239–267. https://doi.org/10.1007/978-3-642-55844-3_11

Knoll, M., Hernández-Guerra, A., Lenz, B., López Laatzen, F., Machín, F., Müller, T. J., & Siedler, G. (2002). The Eastern Boundary Current system between the Canary Islands and the African Coast. *Deep Sea Research Part II: Topical Studies in Oceanography*, *49*(17), 3427–3440. https://doi.org/10.1016/S0967-0645(02)00105-4

Koltermann, K. P, Gouretski, V., & Jancke, K. (2011). Hydrographic Atlas of the World Ocean Circulation Experiment (WOCE). *Volume 3: Atlantic Ocean (Eds. M. Sparrow, P. Chapman and J. Gould). International WOCE Project Office, Southampton, UK*, *2*. https://doi.org/10.21976/C61595

Laiz, I., Pelegrí, J. L., Machín, F., Sangrá, P., Hernández-Guerra, A., Marrero-Díaz, A., & Rodríguez-Santana, A. (2012). Eastern boundary drainage of the north atlantic subtropical gyre. *Ocean Dynamics*, *62*(9), 1287–1310. https://doi.org/10.1007/s10236-012-0560-6

Machín, F., Hernández-Guerra, A., & Pelegrí, J. L. (2006). Mass fluxes in the Canary Basin. *Progress in Oceanography*, *70*(2–4), 416–447.

https://doi.org/10.1016/j.pocean.2006.03.019

Mason, E., Colas, F., Molemaker, J., Shchepetkin, A. F., Troupin, C., McWilliams, J. C., & Sangrà, P. (2011). Seasonal variability of the Canary Current: A numerical study. *Journal of Geophysical Research: Oceans*, *116*(6), 1–20. https://doi.org/10.1029/2010JC006665

McCarthy, J. J., & Carpenter, E. J. (1979). Oscillatoria (*Trichodesmium*) Thebeautii (Cyanophyta) in the central northern Atlantic Ocean. Journal of Phycology, 15(1), 75-82. *Journal of Phycology*, *15*(1), 75–82. https://doi.org/https://doi.org/10.1111/j.1529-8817.1979.tb02965.x

Mompeán, C., Bode, A., Benítez-Barrios, V. M., Domínguez-Yanes, J. F., Escánez, J., & Fraile-Nuez, E. (2013). Spatial patterns of plankton biomass and stable isotopes reflect the influence of the nitrogen-fixer *Trichodesmium* along the subtropical North Atlantic. *Journal of Plankton Research*, *35*(3), 513–525. https://doi.org/10.1093/plankt/fbt011

Neuer, S., Freudenthal, T., Davenport, R., Llinás, O., & Rueda, M. J. (2002). Seasonality of surface water properties and particle flux along a productivity gradient off NW Africa. *Deep-Sea Research Part II: Topical Studies in Oceanography*, *49*(17), 3561–3576. https://doi.org/10.1016/S0967-0645(02)00098-X

Pelegrí, J. L., Arístegui, J., Cana, L., González-Dávila, M., Hernández-Guerra, A., Hernández-León, S., Marrero-Díaz, A., Montero, M. F., Sangrà, P., & Santana-Casiano, M. (2005). Coupling between the open ocean and the coastal upwelling region off northwest Africa: Water recirculation and offshore pumping of organic matter. *Journal of Marine Systems*, *54*, 3–37. https://doi.org/10.1016/j.jmarsys.2004.07.003

Philippart, C. J. M., Anadón, R., Danovaro, R., Dippner, J. W., Drinkwater, K. F., Hawkins, S. J., Oguz, T., O'Sullivan, G., & Reid, P. C. (2011). Impacts of climate change on European marine ecosystems: Observations, expectations and indicators. *Journal of Experimental Marine Biology and Ecology*, *400*(1–2), 52–69. https://doi.org/10.1016/j.jembe.2011.02.023

Ramos, A. G., Martel, A., Codd, G. A., Soler, E., Coca, J., Redondo, A., Morrison, L. F., Metcalf, J. S., Ojeda, A., Suárez, S., & Petit, M. (2005). Bloom of the marine diazotrophic cyanobacterium *Trichodesmium* erythraeum in the Northwest African Upwelling, *301*, 303–305.

Ratsimandresy, A., Pelegrí, J. L., Marrero-Díaz, A., Hernández-Guerra, A., & Martínez, A. (2001). Seasonal variability of the upper warmwatersphere in the Canary Basin. *Scientia*

Marina, *65*(Suppl. 1), 251–258. https://doi.org/10.3989/scimar.2001.65s1251

Ricciardulli, l. and Wentz, F. (2011). Reprocessed QuikSCAT (V04) Wind Vectors with Ku-2011 Geophysical Model Function. Remote Sensing Systems Tech Rep. 043011

Stramma, L. (1984). Geostrophic transport in the Warm Water Sphere of the eastern subtropical North Atlantic. *Journal of Marine Research*, *42*(3), 537–558. https://doi.org/10.1357/002224084788506022

Stramma, L., & Siedler, G. (1988). Seasonal changes in the North Atlantic subtropical gyre. *Journal of Geophysical Research*, *93*(C7), 8111. https://doi.org/10.1029/JC093iC07p08111

Schulzweida, U. (2018). Max Planck Institute for Meteorologie, Climate Data Operators (CDO) User Guide, Version 1.9.3, , https://code.mpimet.mpg.de/projects/cdo/embedded/cdo.pdf.

Talley, L. D., Pickard, G. L., Emery, W. J., & Swift, J. H. (2011). Atlantic Ocean. In *Descriptive Physical Oceanography* (pp. 1–43). https://doi.org/10.1016/B978-0-7506-4552-2.10021-6

Troupin, C., MacHín, F., Ouberdous, M., Sirjacobs, D., Barth, A., & Beckers, J. M. (2010). High-resolution climatology of the northeast Atlantic using Data-Interpolating Variational Analysis (Diva). *Journal of Geophysical Research: Oceans*, *115*(8), 1–20. https://doi.org/10.1029/2009JC005512

Tyrrell, T., Marañón, E., Poulton, A. J., Bowie, A. R., Harbour, D. S., & Woodward, E. M. S. (2003). Large-scale latitudinal distribution of *Trichodesmium* spp. in the Atlantic Ocean. *Journal of Plankton Research*, *25*(4), 405–416. https://doi.org/10.1093/plankt/25.4.405

Van Camp, L., Nykjaer, L., Mittelstaedt, E., & Schlittenhardt, P. (1991). Upwelling and boundary circulation off Northwest Africa as depicted by infrared and visible satellite observations. *Progress in Oceanography*, *26*(4), 357–402. https://doi.org/10.1016/0079-6611(91)90012-B

Vélez-Belchí, P., Carballo Gonzalez, M., Perez-Hernández, M. D., & Hernández-Guerra, A. (2015). In *Open ocean temperature and salinity trends in the Canary Current Large Marine Ecosystem*. L. Valdés & I. Déniz González, (Eds.), *Oceanographic and biological features in the Canary Current Large Marine Ecosystem* (IOC Techni, Vol. 115). Paris. Retrieved from uri: http://hdl.handle.net/1834/9196. 2015%0AOPEN

Villagarcia Ubeda, M.G., Cianca, A., Barrera Rodriguez, C., Rueda Lopez, M.J., Llinás, O., (2018). IS14B-2563: *Observation of two mesoscale events anomalies within ESTOC time-series.* Ocean Sciences Meeting, Portland, Oregon, USA.

Appendix A

Validation of SODA versus other data sets

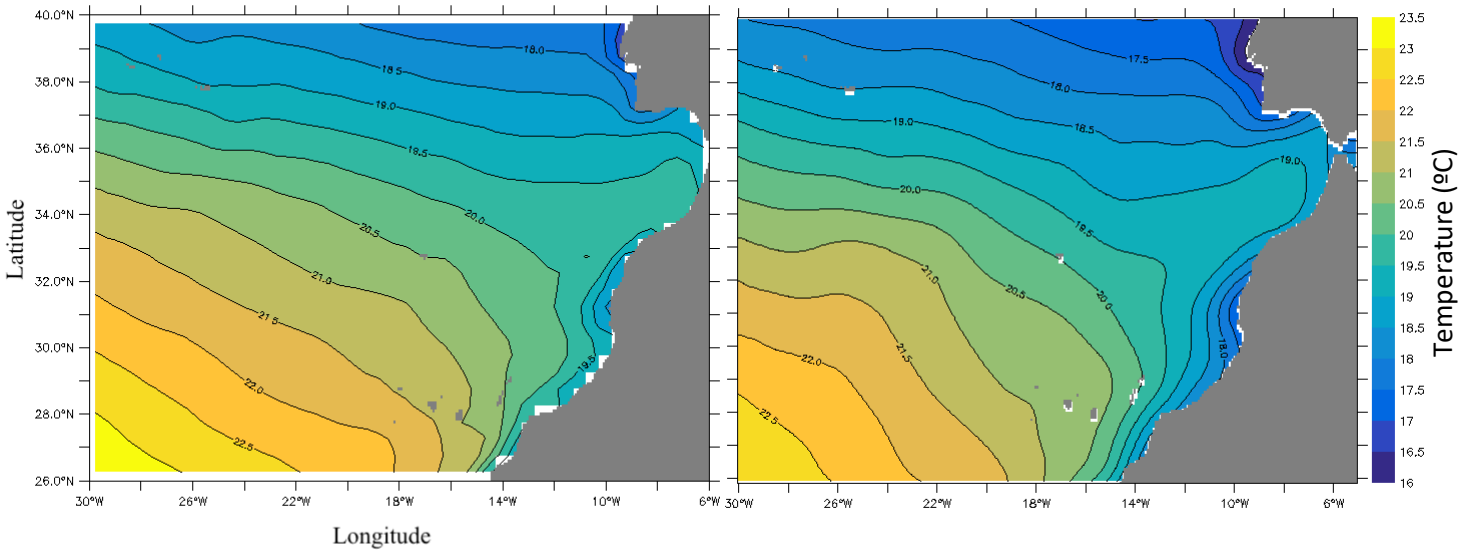

Figure 1A. Mean sea surface temperature (ºC) of the Canary Basin for a) SODA reanalysis climatological year and b) DIVA climatology.

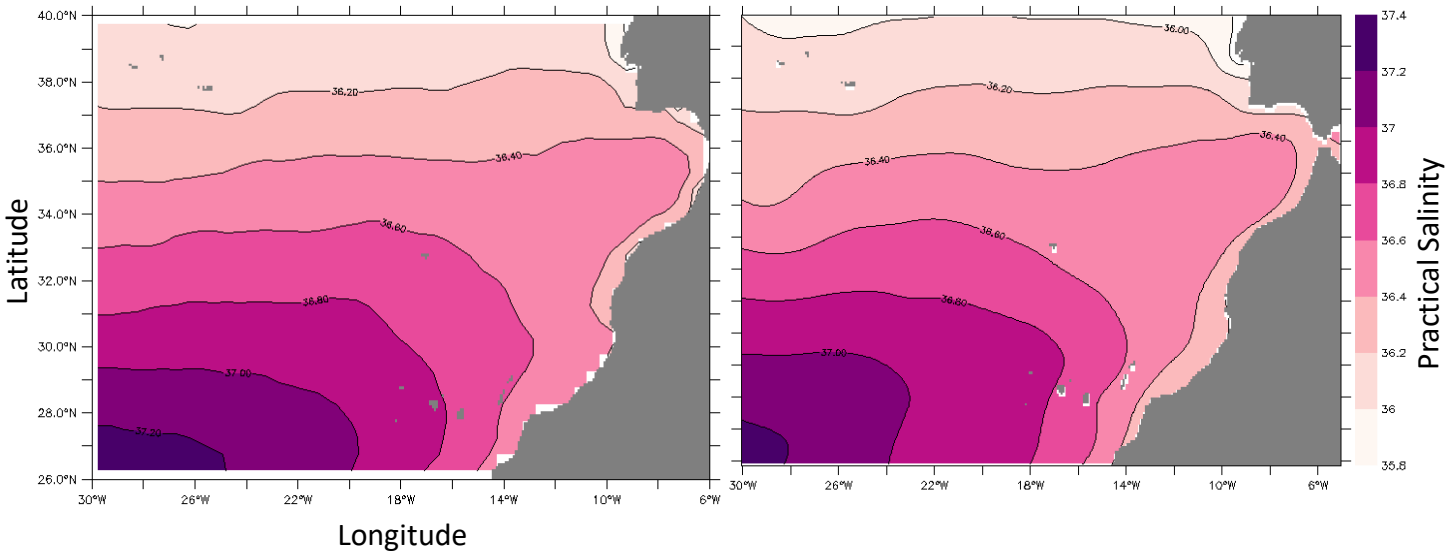

Figure 2A. Mean sea surface salinity of the Canary Basin for a) SODA reanalysis climatological year, b) DIVA climatology.

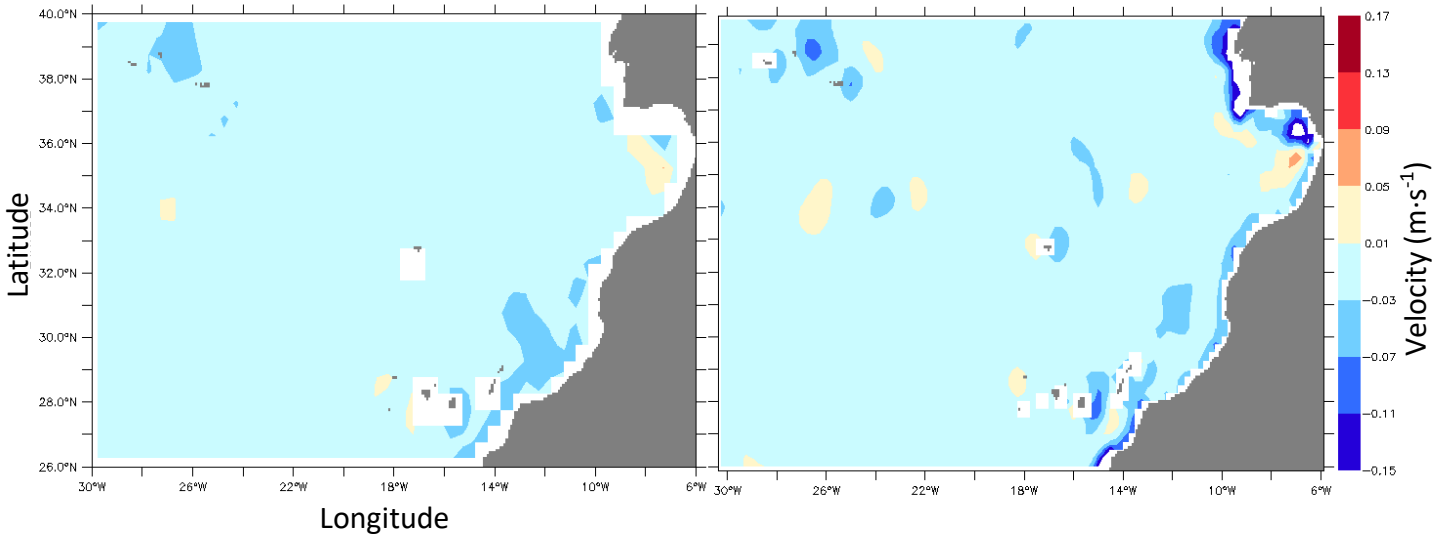

Figure 3A. Mean meridional component of the velocity ($m \cdot s^{-1}$) over the Canary Basin at 5m for a) SODA reanalysis climatological year and b) DIVA climatology

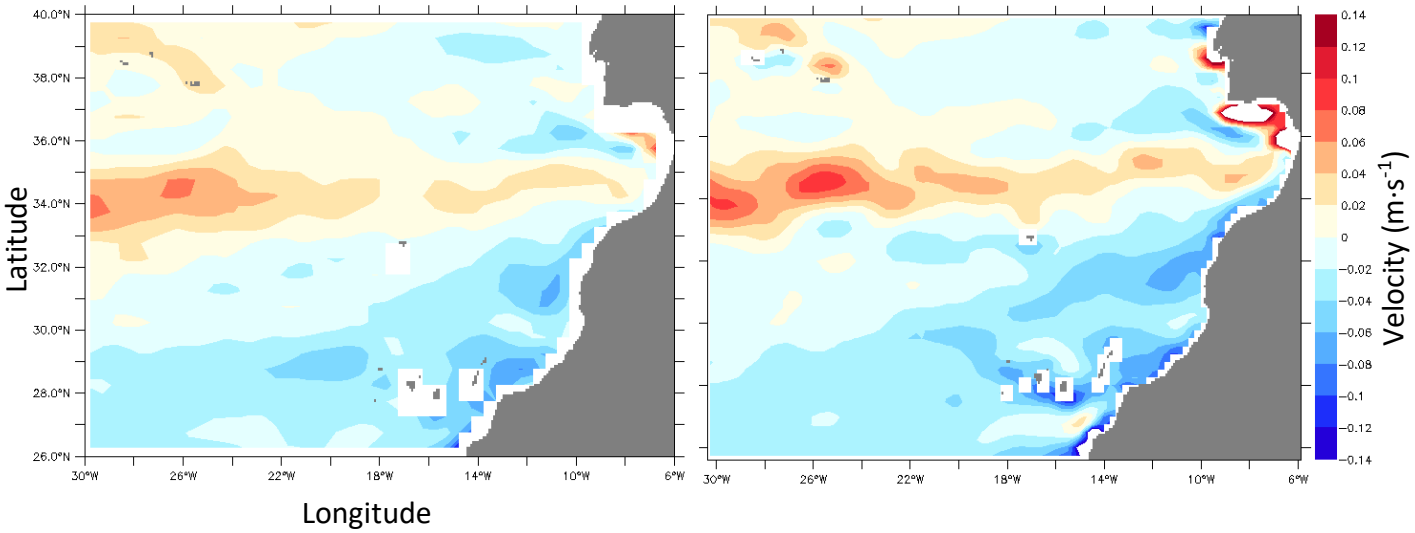

Figure 4A. Mean zonal component of the velocity ($m \cdot s^{-1}$) over the Canary Basin at 5m for a) SODA reanalysis climatological year and b) DIVA climatology

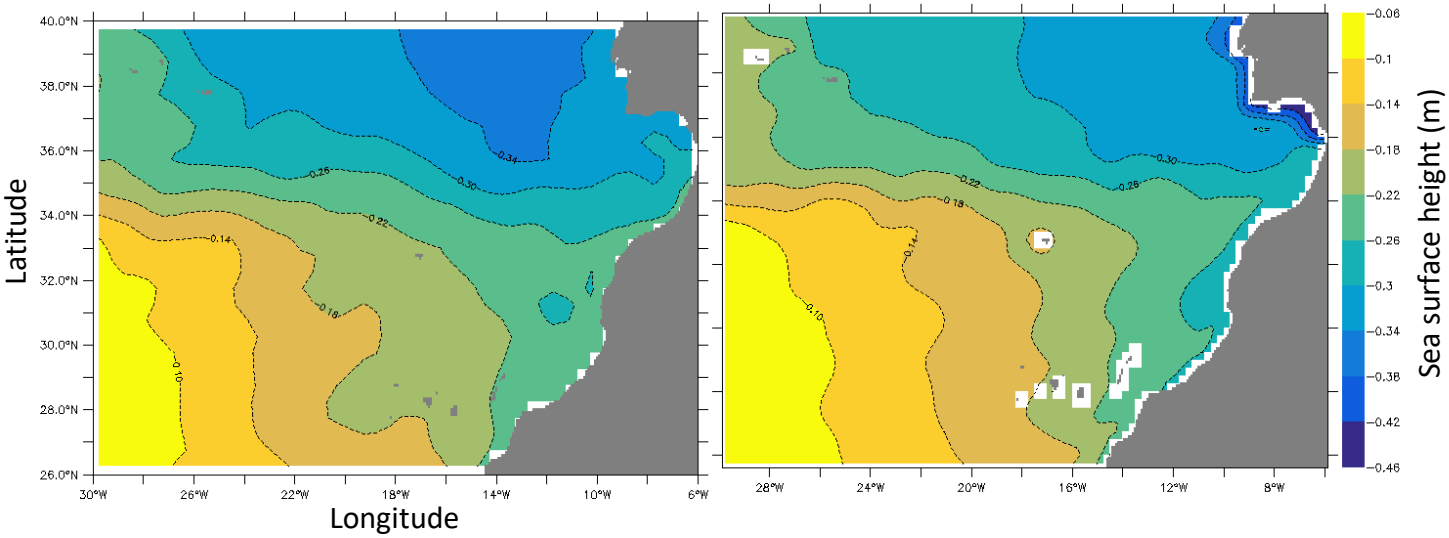

Figure 5A. Mean sea surface height (m) of the Canary Basin for a) SODA reanalysis climatological year and b) DIVA climatology

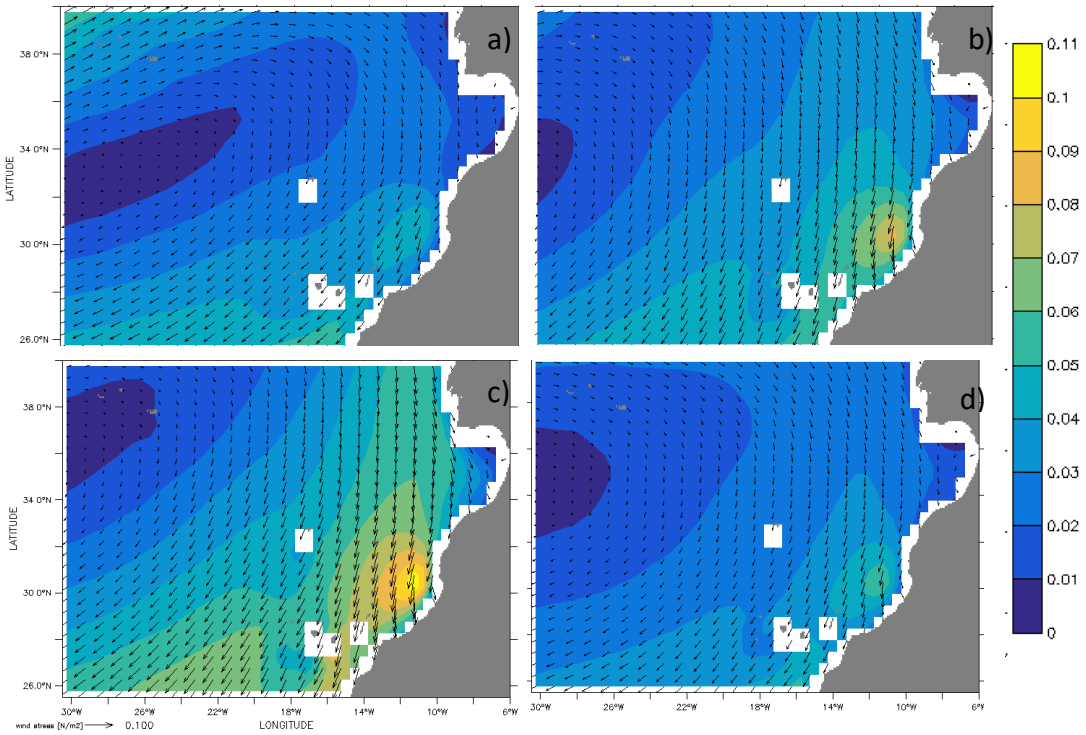

Figure 6A. SODA Wind stress regime for a) winter, b) spring, c) summer, d) autumn. Color key indicates wind stress intensity ($N \cdot m^2$), arrow direction indicates wind stress direction arrow length indicate wind stress magnitude.

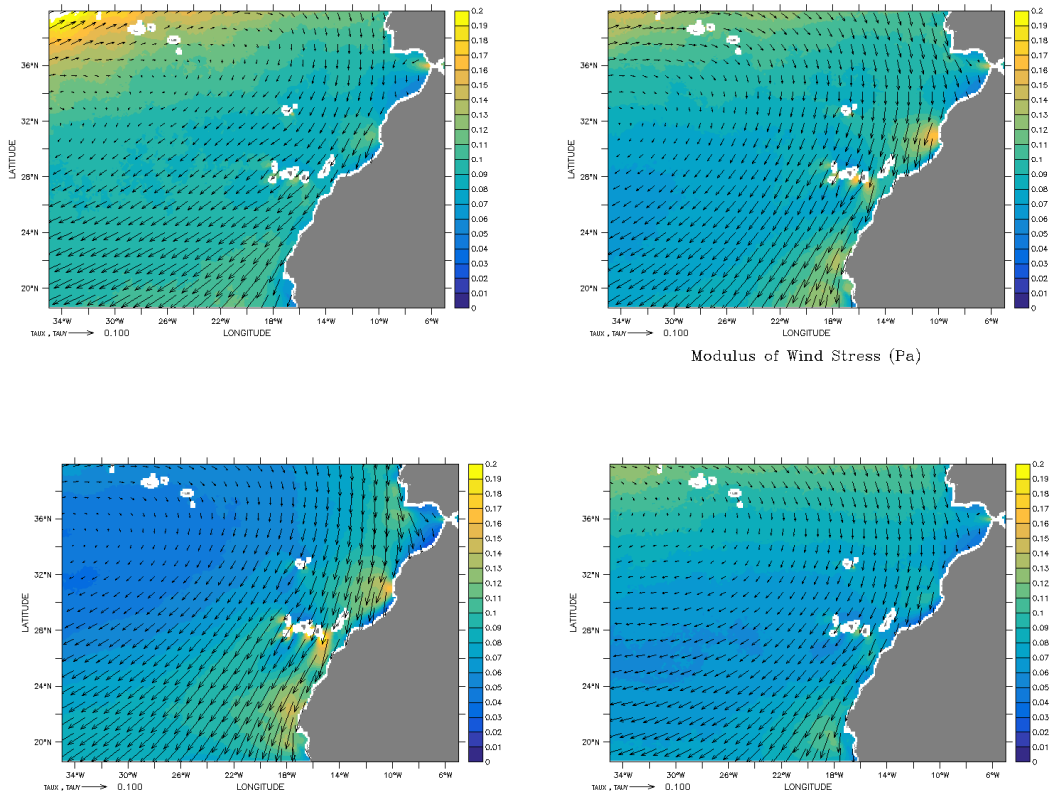

Figure 7A: Wind stress ($N \cdot m^2$) field for QuickScat for up left to up right, down left down right = Winter, Spring, Summer, autumn

Appendix B

Results

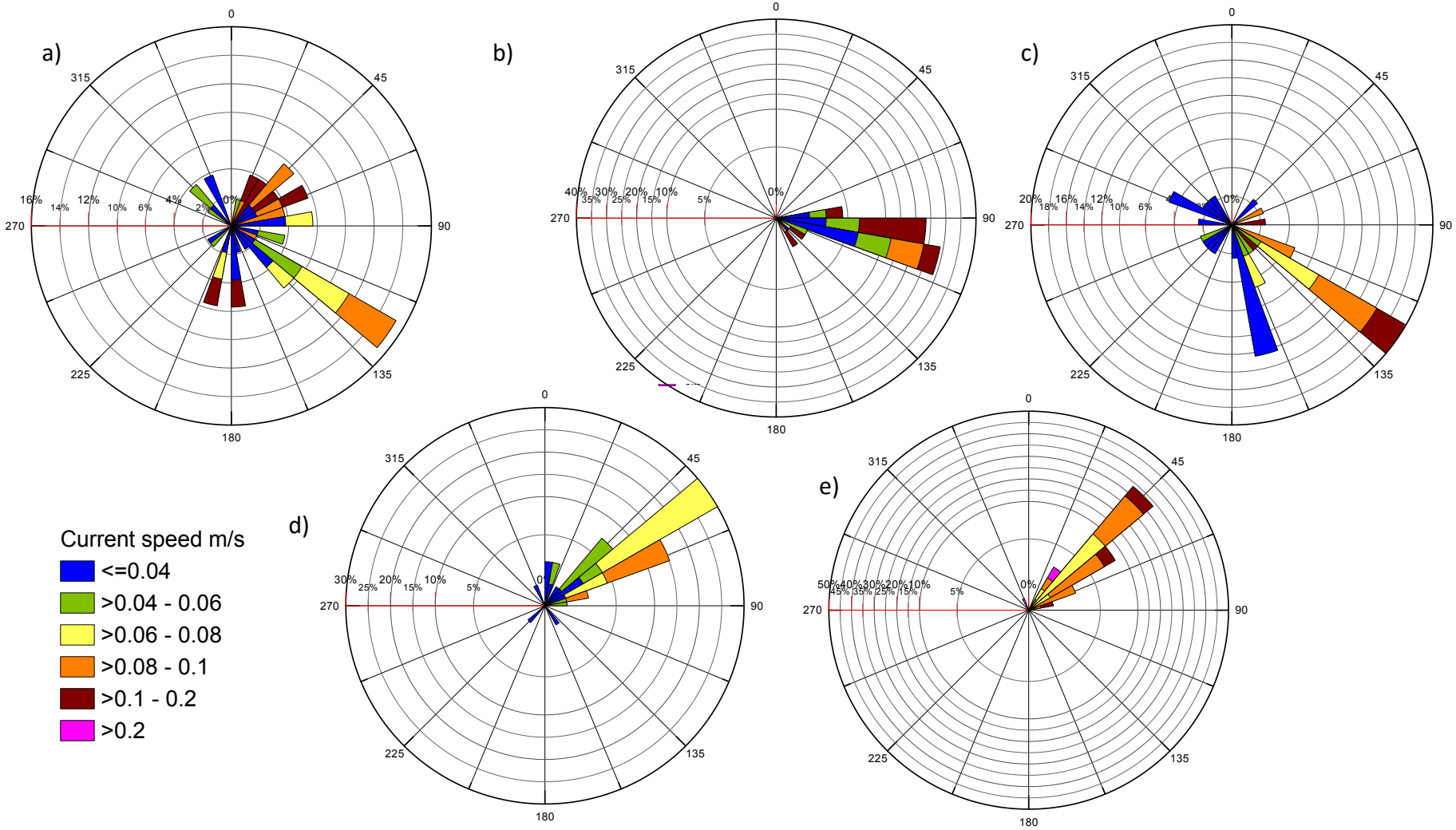

Figure 1B. ADCP measured directions (degrees) and intensities ($m \cdot s^{-1}$) (color key) for a) April and May, b) June, c) July, d) August and e) September. 20-100 m depth averaged.

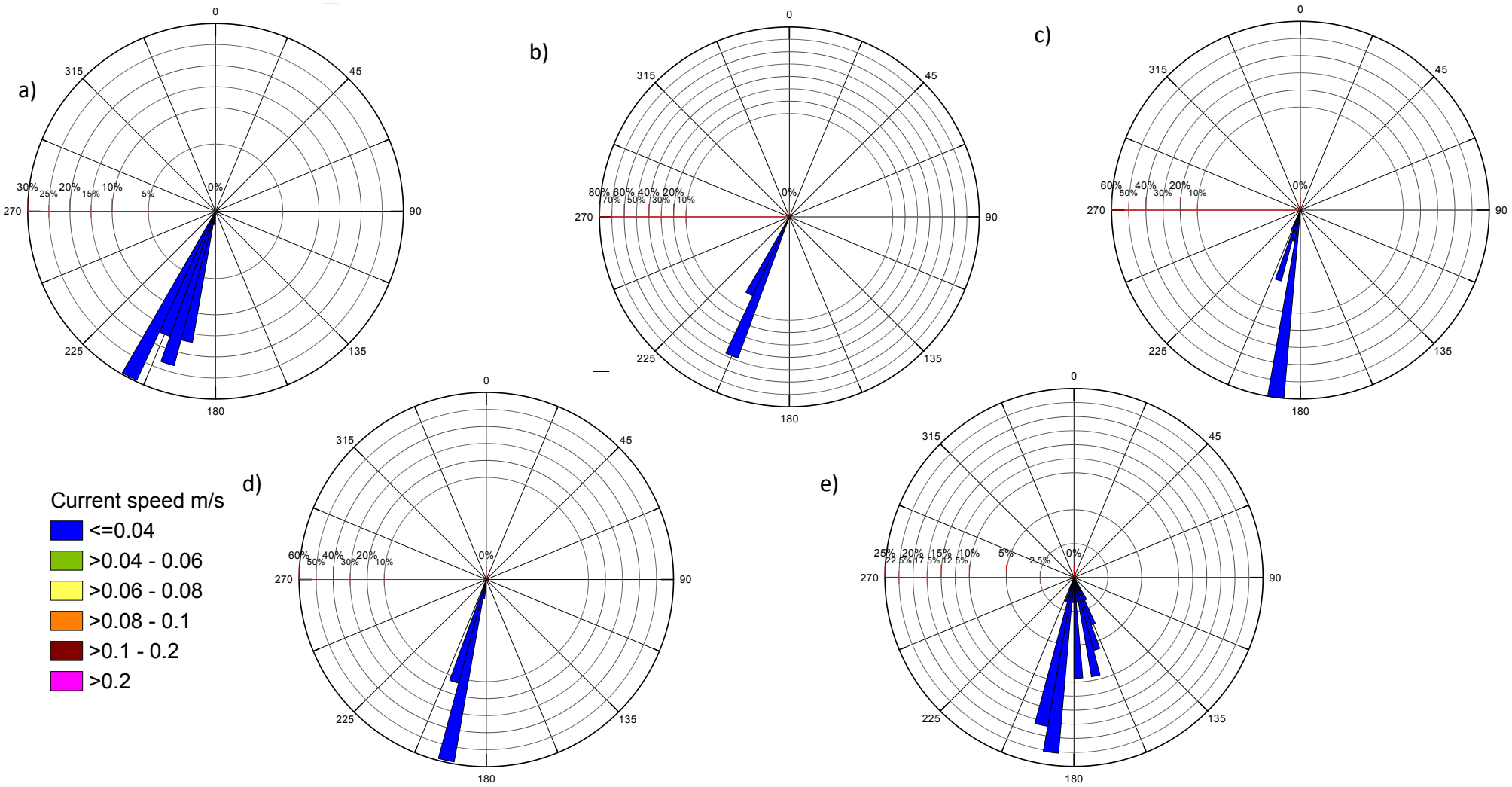

Figure 2B: SODA climatological directions (degrees) and intensities ($m \cdot s^{-1}$) (color key) for a) April and May, b) June, c) July, d) August and e) September. 20-100 m depth averaged

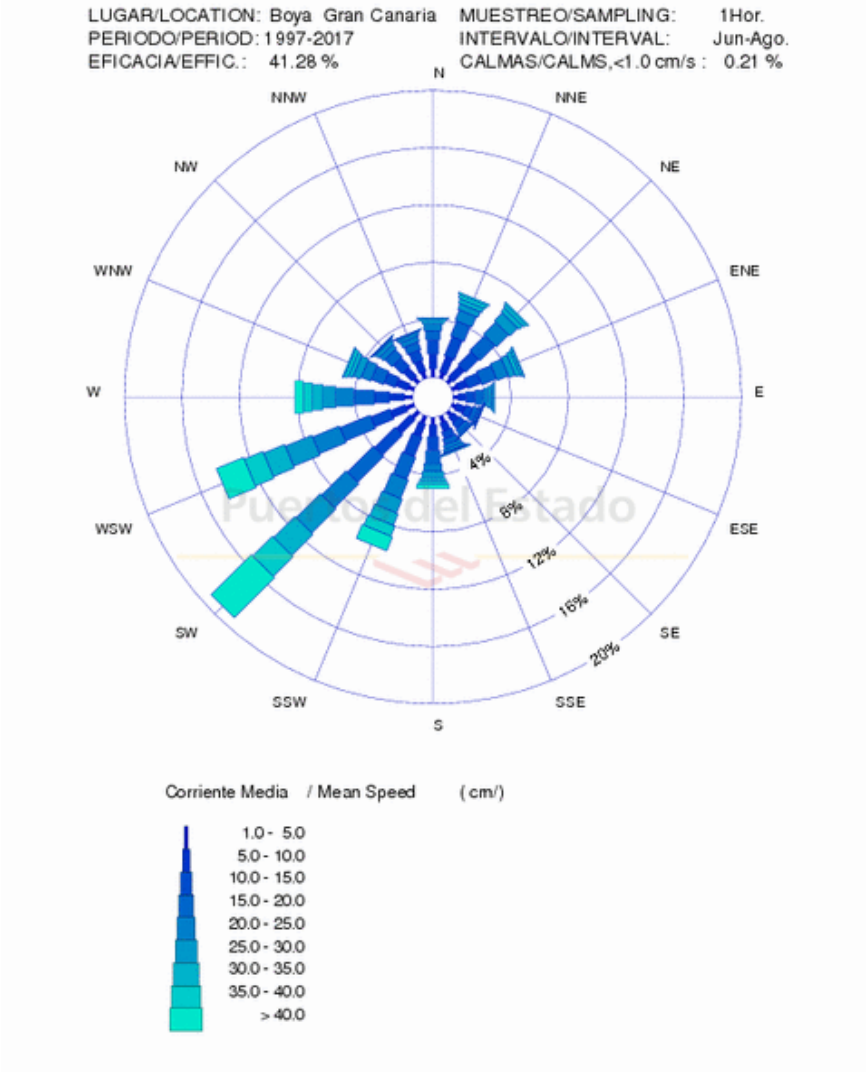

Figure 3B. Mean current direction and intensity for summers (Jun-August) 1997-2017. Surface buoy belonging to Puertos del Estado, Gran Canaria coast.

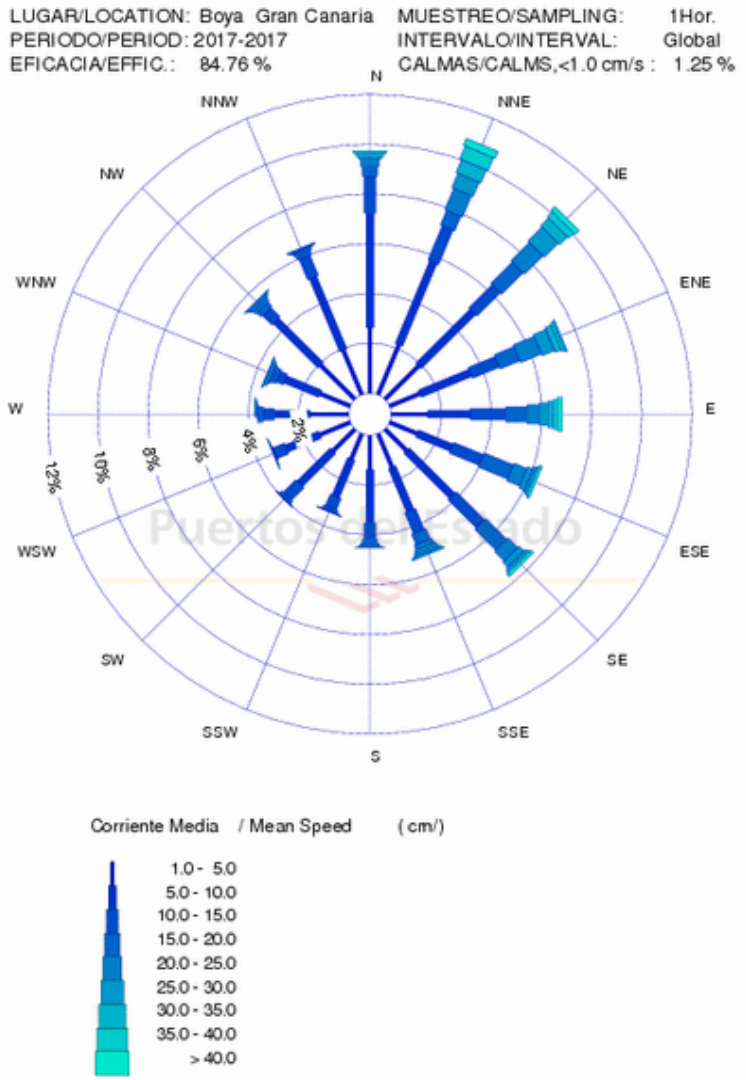

Figure 4B. Mean current direction and intensity for summer 2017 (June-August). Surface buoy belonging to Puertos del Estado, Gran Canaria coast.

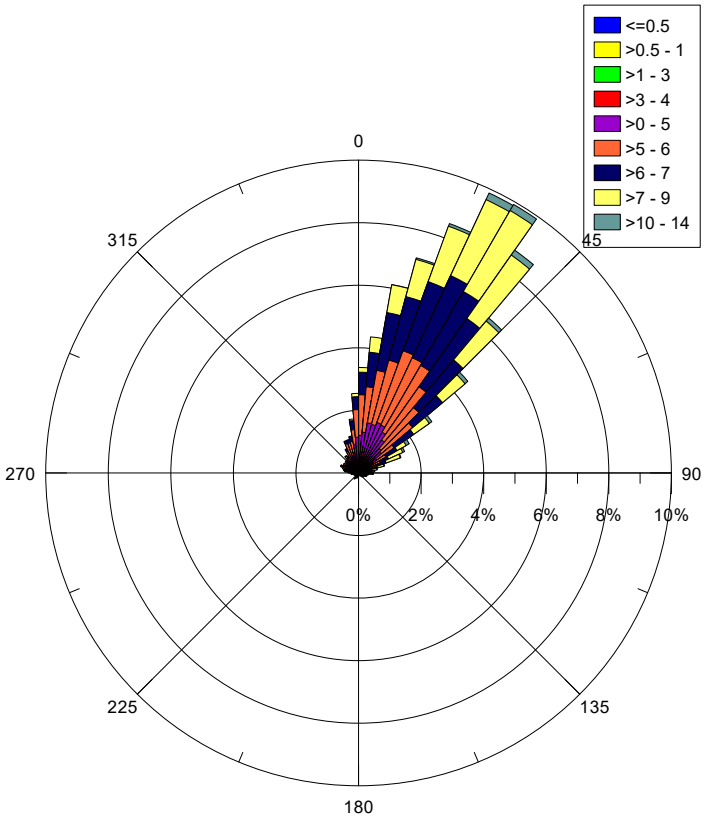

Figure 5B. Wind directions and intensities recorded at the ESTOC position (29.2ºN,15.5ºW) from mid-April to late-September. Direction are given in degrees (0º= northerly, 90º= easterly, 180º= southerly,270º= westerly) and intensities in m/s (<0.5 $m \cdot s^{-1}$ - 14 $m \cdot s^{-1}$).

SODA climatological year for temperature (ºC)

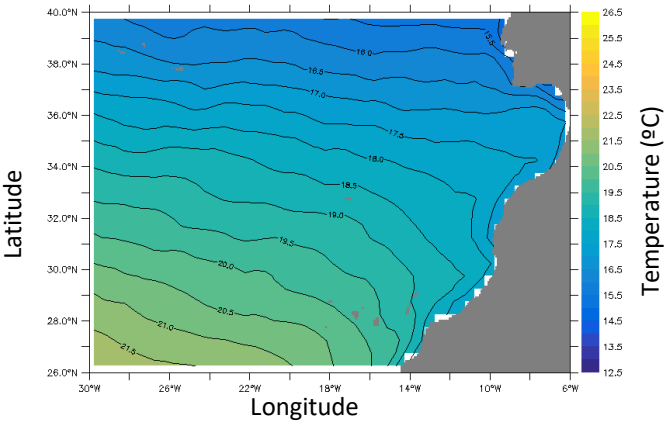

Figure 1C. January

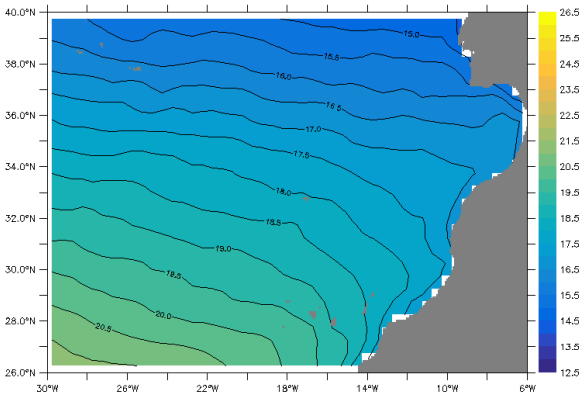

Figure 2C. February

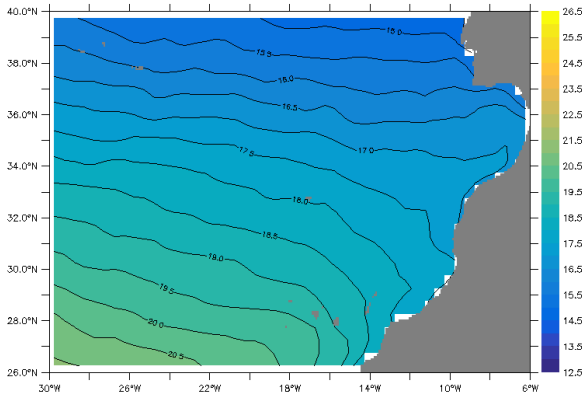

Figure 3C. March

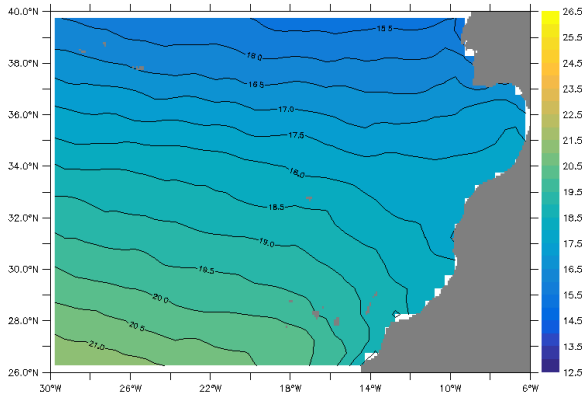

Figure 4C. April

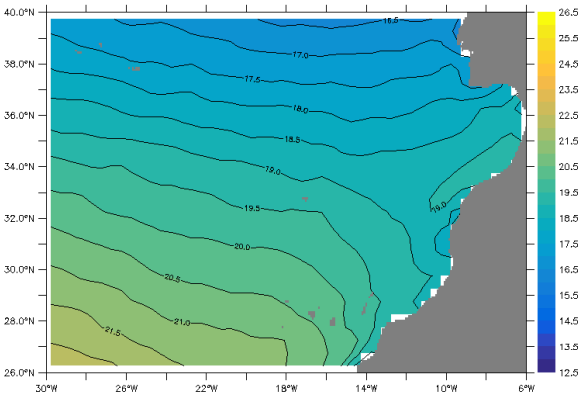

Figure 5C. May

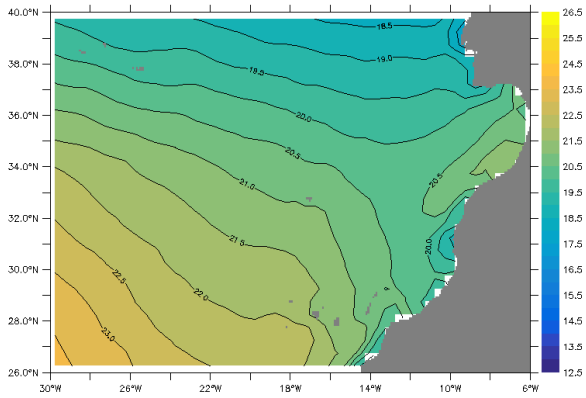

Figure 6C. June

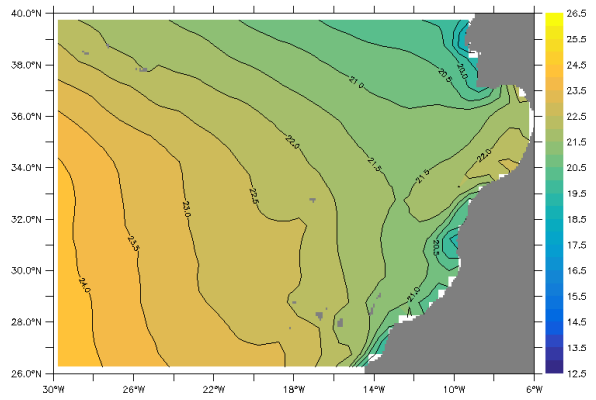

Figure 7C. July

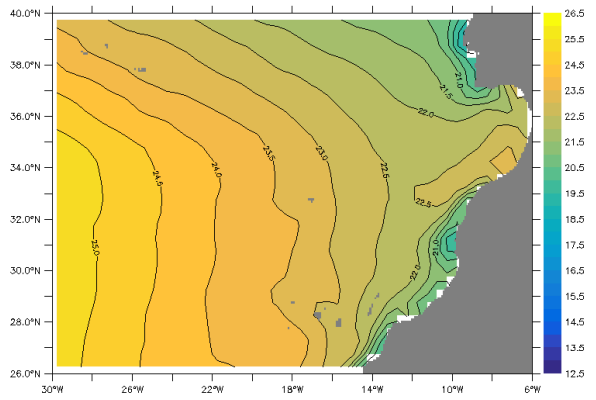

Figure 8C. August

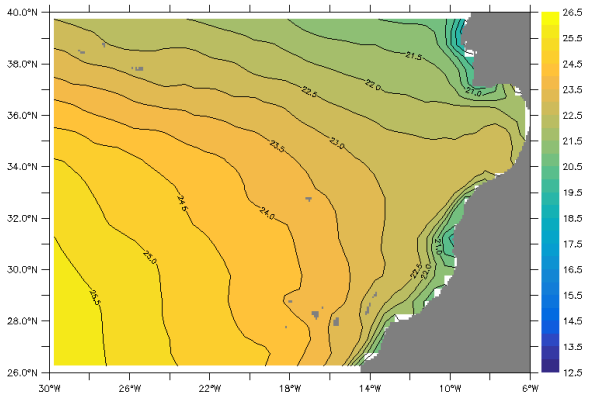

Figure 9C. September

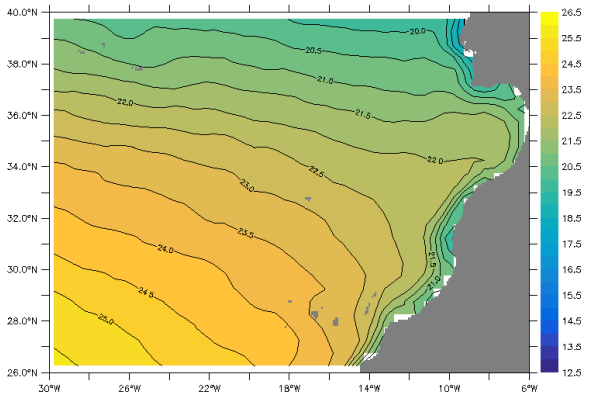

Figure 10C. October

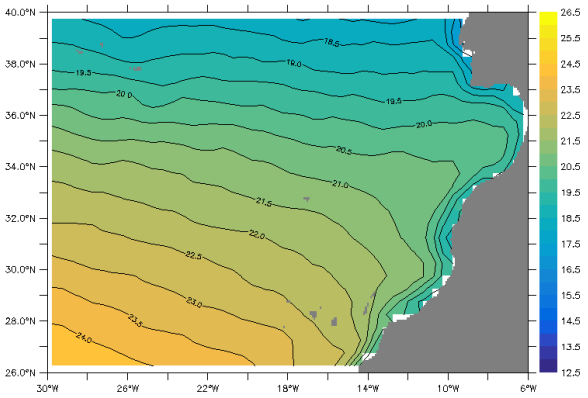

Figure 11C.November

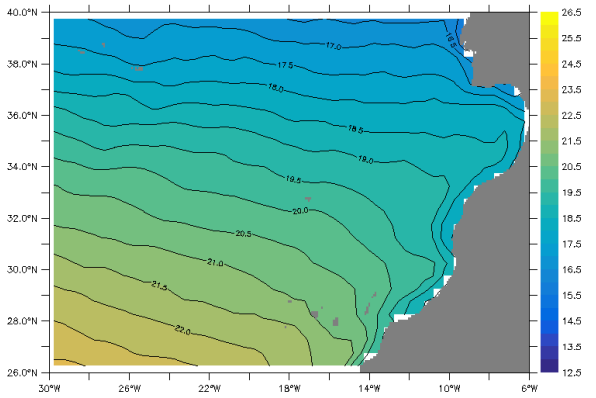

Figure 12. C December